UNCLASSIFIED

ORNL 875
Series A

8A

MARTIN MARIETTA ENERGY SYSTEMS LIBRARIES
3 4456 0352688 8

THE TOTAL NEUTRON CROSS SECTIONS OF Ni^{58} AND Ni^{60}

C.P. STANFORD

OAK RIDGE NATIONAL LABORATORY
CENTRAL RESEARCH LIBRARY
CIRCULATION SECTION
4500N ROOM 175
LIBRARY LOAN COPY
DO NOT TRANSFER TO ANOTHER PERSON
If you wish someone else to see this report, send in name with report and the library will arrange a loan.
UCN-7969 (3 9-77)

OAK RIDGE NATIONAL LABORATORY
OPERATED BY
CARBIDE AND CARBON CHEMICALS DIVISION
UNION CARBIDE AND CARBON CORPORATION
UCC
POST OFFICE BOX P
OAK RIDGE, TENNESSEE

UNCLASSIFIED

UNCLASSIFIED

ORNL-875

This document consists of 58 pages.
Copy 8 of 195. Series A

Contract No. W-7405, eng 26

PHYSICS DIVISION

THE TOTAL NEUTRON CROSS SECTIONS OF Ni^{58} AND Ni^{60}

C. P. Stanford

DATE ISSUED DEC 11 1950

OAK RIDGE NATIONAL LABORATORY
operated by
CARBIDE AND CARBON CHEMICALS DIVISION
Union Carbide and Carbon Corporation
Post Office Box P
Oak Ridge, Tennessee

* A thesis submitted to the Committee on Graduate Study of the University of Tennessee in partial fulfillment of the requirements for the degree of Master of Science, August, 1950.

UNCLASSIFIED

MARTIN MARIETTA ENERGY SYSTEMS LIBRARIES

3 4456 0352688 8

Internal Distribution:

1	G. T. Felbeck (C&CCD)
2-3	706-A Library
4	706-B Library
5	Biology Library
6	Health Physics Library
7	Metallurgy Library
8-9	Training School Library
10-13	Central Files
14	C. E. Center
15	C. E. Larson
16	W. B. Humes (K-25)
17	W. D. Lavers (Y-12)
18	A. M. Weinberg
19	J. A. Swartout
20	E. J. Murphy
21	F. C. VonderLage
22	A. H. Snell
23	E. H. Taylor
24	A. Hollaender
25	F. L. Steahly
26	K. Z. Morgan
27	D. W. Cardwell
28	M. T. Kelley
29	W. H. Pennington
30	E. O. Wollan
31	L. D. Roberts
32	A. S. Householder
33	J. A. Lane
34	R. N. Lyon
35	M. M. Mann
36	W. C. Koehler
37	W. K. Ergen
38	E, P. Blizard
39	S. Bernstein
40	M. J. Skinner
41-106	C. P. Stanford
107	Central Files (O.P.)

External Distribution:

108-115	Argonne National Laboratory
116	Armed Forces Special Weapons Project
117-118	Atomic Energy Commission, Washington
119	Battelle Memorial Institute
120	Brush Beryllium Company
121-128	Brookhaven National Laboratory
129	Bureau of Ships
130-133	Carbide & Carbon Chemicals Division (K-25)
134-137	Carbide & Carbon Chemicals Division (Y-12)
138	Chicago Operations Office
139	Columbia University (J. R. Dunning)
140-142	General Electric, Richland
143	Idaho Operations Office
144-145	Iowa State College
146-149	Knolls Atomic Power Laboratory
150-152	Los Alamos Scientific Laboratory
153	Massachusetts Institute of Technology (A. Kaufmann)
154-156	Mound Laboratory
157-158	National Advisory Committee for Aeronautics
159-160	National Bureau of Standards
161-165	New York Operations Office
166	North American Aviation, Inc.
167	Patent Branch (Washington)
168	Sandia Laboratory
169-183	Technical Information Division (Oak Ridge)
184-185	USAF, NEPA
186-190	University of California Radiation Laboratory
191-194	Westinghouse Electric Company
195	Santa Fe Operations Office

ACKNOWLEDGMENT

I wish to thank Dr. S. Bernstein for his constant aid and advice in the planning, execution, and interpretation of this experiment. This work was part of a larger program, carried out under his direction, for the measurement of the total neutron cross sections of small quantities of certain rare stable and radioactive isotopes as a function of energy. Mr. T. E. Stephenson and Mr. J. B. Dial also participated in this program.

The samples of separated nickel isotopes used in this work were prepared by the Isotopes Production Division of the Electromagnetic Separation Plant, Carbide and Carbon Chemicals Corporation at Oak Ridge, Tennessee. Mr. D. LaValle of the Chemistry Division of Oak Ridge National Laboratory assayed the samples for water content.

TABLE OF CONTENTS

CHAPTER		PAGE
I.	INTRODUCTION	7
II.	DESCRIPTION OF THE EXPERIMENT	8
III.	INSTRUMENT PERFORMANCE	15
IV.	EXPERIMENTAL DATA	35
V.	DISCUSSION OF EXPERIMENTAL RESULTS	46

LIST OF TABLES

TABLE		PAGE
I.	Sample Analyses	36
II.	Determination of Cross Section of $Ni^{58}O$ from Measured Transmission of Sample	37
III.	Neutron Energy Determination from the Crystal Angle	40
IV.	Calculation of Statistical Error	44
V.	Energy Location of Crystalline Scattering Cross Section Discontinuities for NiO	49

LIST OF FIGURES

FIGURE		PAGE
1.	A Type of Spectrograph Suggested by Du Mond and Kirkpatrick in Which Accurate Focusing May be Obtained	11
2.	Principle of a Bent Crystal Focusing Spectrograph According to Johann	11
3.	The Bent Crystal Spectrometer	16
4.	Neutron Spectrometer Diagram	17
5.	Sample Positioning Mechanism	18
6.	Sample Shifter Showing Wafer in Place	19
7.	Sample Tube Holder	21
8.	Absolute Counting Rate vs. Energy for Two mm Capillary and Six mm Slit Width	22
9.	Background vs. Energy 6 mm Slit Width	23
10.	Beam Count/Background	24
11.	Counting Rate vs. Crystal Curvature (5 mm Slit Width)	25
12.	Counting Rate vs. Slit Width	26
13.	Rocking Curves (6 mm Slit)	28
14.	Ratio $\frac{\text{Counts/Sec E}}{\text{Counts/Sec W}}$	29
15.	Cadmium Cross Section vs. Energy Measured by Two Tube Method	31
16.	Absorption of Reflected Beam in BF_3	32
17.	Schematic Circuit Diagram	34
18.	Total Cross Section of $Ni^{58}O$	42
19.	Total Cross Section of $Ni^{60}O$ Corrected for Water Impurity	43
20.	Scattering Resonance	54

CHAPTER I

INTRODUCTION

Normal nickel was shown to have anomalously high scattering cross section for neutrons.[1] Further evidence is given by the total cross section measurements of Rainwater *et al.*[2], and absorption cross section measurement of Pomerance.[3] The results of these observers are 19 barns (1 barn = 10^{-24} cm^2) for the total cross section and 4.8 barns for the absorption cross section. The difference between these two values is the scattering cross section, 14 barns.

Separated nickel isotopes have recently become available in amounts sufficient to permit investigation of their total neutron cross section as a function of neutron energy. In an attempt to determine which nickel isotope is responsible for the high scattering cross section, the total cross section of $Ni^{58}O$ and $Ni^{60}O$ was measured as a function of neutron energy between 0.025 and 0.5 e.v. The chain reactor at Oak Ridge National Laboratory was used as a source for a highly collimated beam of neutrons. Monochromatic neutrons were procured by reflecting this continuous incident distribution from a crystal. By the Bragg relation a given glancing angle corresponds to a definite neutron wave length or energy.

---

[1] C. G. Shull and E. O. Wollan, unpublished work.

[2] L. J. Rainwater, W. J. Havens, C. S. Wu and C. L. Meaker, *Reviews of Modern Physics*, 19:276, 1947.

[3] H. Pomerance and J. I. Hoover, MDDC-1626, p. 8, 1947.

CHAPTER II

DESCRIPTION OF THE EXPERIMENT

The De Broglie wave length of a particle is

$$\lambda = \frac{h}{m\ v} \tag{1}$$

where h is Planck's constant, m is the mass of the particle and v the particle velocity.

The kinetic energy of the particle is

$$E = 1/2\ m\ v^2 \tag{2}$$

As $m\ v = \sqrt{2\ m\ E}$, it follows that,

$$\lambda = \frac{h}{\sqrt{2\ m\ E}} \tag{3}$$

The wave properties of particles permit the selection of a beam of monoergic neutrons by means of crystal diffraction. This technique is simpler for neutrons than for most other particles since the neutron has no change. Bragg's law states:

$$n\ \lambda = 2\ d\ \sin\theta \tag{4}$$

where n is an integer and represents the order of diffraction, λ is the wave length, and d is the distance between a given set of planes of the crystal. θ is the glancing angle, or the complement of the angle of incidence of optical nomenclature. Bragg's law states that for a given scattering angle there will be found in the reflected beam the energies E_1, $4E_1$, $9E_1$, etc. corresponding to orders of diffraction, $n = 1, 2, 3$. Under favorable experimental conditions the effect of higher order reflections may be negligible. (These conditions are discussed below.)

Throughout this work use has been made of reflections from the (100) planes of a 5 inch by 1 inch by 1 millimeter quartz crystal. Quartz is a hexagonal crystal.[1] The grating space d of a parallel set of planes is given by[2]

$$d = \frac{1}{\sqrt{\frac{4}{3a^2}(h^2 + hk + k^2) - \frac{l^2}{c^2}}} \tag{5}$$

where $a = 4.903$, $c = 5.393$[3] and (hkl) are the Miller indices of the planes.[4]

With equation (5) and the Miller indices (100) we obtain

$$d = 4.24\ A \tag{6}$$

Substituting this value in (4) and using equation (3) gives for $n = 1$ (see page 30 of this thesis)

$$E = \frac{1.136 \times 10^{-3}}{\sin^2 \theta} \tag{7}$$

There are numerous methods of obtaining a nearly monochromatic beam from a finite source by means of crystal diffraction. If the crystal is plane, one must have a well collimated beam in order to define precisely the glancing angle. Such an arrangement results in low intensity because of the small solid angle subtended by the crystal at the source. With a source of small dimensions, crystal focusing may be used to concentrate the diffracted rays and to reduce their energy spread.[5] Du Mond and Kirkpatrick[6] have shown that if the crystal is both ground and bent, a perfectly focused monochromatic beam may be obtained from a point source. The source, crystal and detector

---

[1] Martin Buerger, *X-ray Crystallography* (New York: John Wiley and Sons, Inc. 1912), p. 334.

[2] *Ibid.*, p. 103.

[3] *Handbook of Chemistry and Physics* (Cleveland, Ohio: Chemical Rubber Publishing Company, 1949), p. 2076.

[4] C. F. Meyer, *The Diffraction of Light, X-rays and Material Particles* (Chicago, Illinois: The University of Chicago Press, 1934), p. 291.

[5] *Ibid.*, pp. 750-756.

[6] J. W. M. Du Mond and H. A. Kirkpatrick, "The Multiple Crystal X-Ray Spectrograph," *Review of Scientific Instruments*, 1:88, 1930.

determine a circle as shown in Figure 1. The crystal is equidistant from source and detector. The crystal is bent with a radius of curvature equal to the diameter of the above circle. The crystal surface is then ground to coincide with the smaller circle. The rays from any point source *A* on the smaller circle that obey the Bragg law will then come to focus at point *B* on the same circle.

H. H. Johann[7] developed a curved crystal X-ray spectrometer which gave imperfect but "adequate" focusing, using the principles of the Rowland circle of optics, in which the crystal was bent but not ground. This is illustrated in Figure 2.

For neutron work with a chain reactor the source is necessarily fixed. Since shielding of neutron detectors is bulky, it is also inconvenient to move the "grating." In our apparatus we use the approximate focus of Johann. The source and detector are equally distant from the crystal. The conditions of the Rowland circle and Bragg's law are satisfied for each energy setting by varying the curvature of the crystal until the best focusing is procured.

The measurement of total neutron cross sections as a function of neutron energy is accomplished by preparing a sample of known composition and of physical size sufficient to intercept all of the neutron beam. Measurements are taken of the beam intensity with and without the sample in the beam. Background measurements are also taken which must be subtracted from the beam counts. The background is due to all sources of neutrons other than coherent Bragg scattering, such as diffuse scattering from the crystal and crystal holder, stray neutrons from other nearby sources, and spurious "neutrons" of electronic origin. The background is measured by simply rotating the crystal off the Bragg peak by one degree, the counter angle remaining fixed.

The four measured counting rates are:

r_0 = incident beam

r_1 = transmitted beam

r_2 = incident beam background

r_3 = transmitted beam background

---

[7] H. H. Johann, "Die Erzeugung lichtstarker Rontgenspektren mit Hilfe von Konkavkristallen," *Zeitschrift Fur Physick*, 69:185, 1931.

UNCLASSIFIED
DWG. 9336

FIG. 1

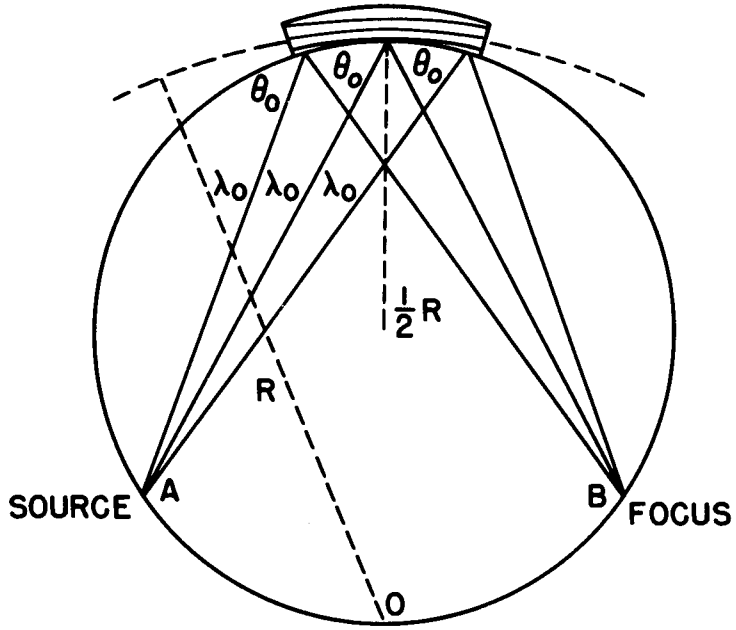

A TYPE OF SPECTOGRAPH SUGGESTED BY DU MOND AND KIRKPATRICK IN WHICH ACCURATE FOCUSSING MAY BE OBTAINED

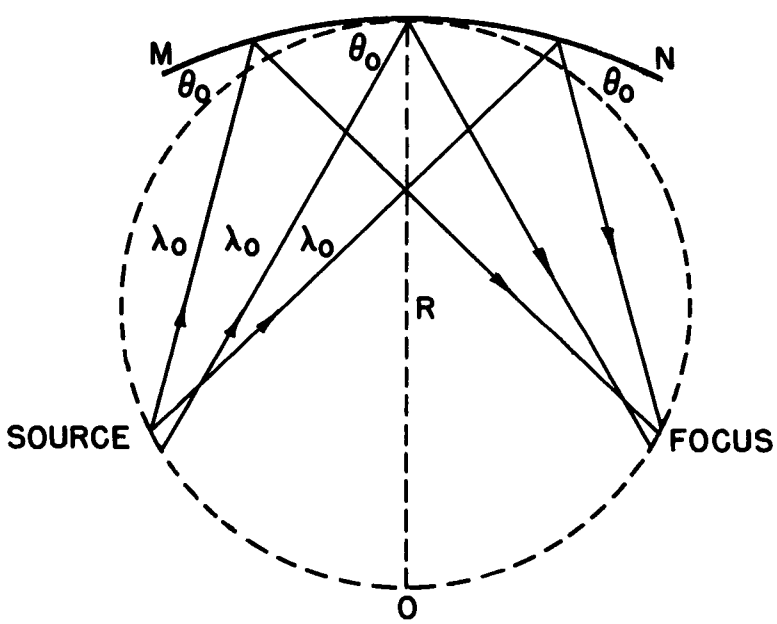

PRINCIPLE OF A BENT CRYSTAL FOCUSSING SPECTOGRAPH ACCORDING TO JOHANN
FIG. 2

We have

$$r_i = \frac{c_i}{t_i} \tag{8}$$

where c_i and t_i are the total counts and counting time for the ith counting rate. The transmission T can then be written as

$$T = \frac{r_1 - r_3}{r_0 - r_2} \tag{9}$$

Assuming that a single scattering is sufficient to remove the neutron from the beam, then the fraction dI/I of the intensity I of a beam of neutrons removed as they pass through a layer of material is proportional to the thickness dt of this layer, the number of molecules per cubic centimeter, n, and the total cross section σ per molecule. Then

$$dI/I = n \sigma d t \tag{10}$$

This equation gives on integration

$$ln\ I = - n t \sigma + ln\ I_0 \tag{11}$$

taking $ln\ I_0$ as the constant of integration. This may be written

$$ln\ I/I_0 = - n t \sigma \tag{12}$$

or

$$I = I_0 e^{-n t \sigma} \tag{13}$$

where I_0 represents the incident intensity of neutrons and I the intensity after traversing a layer of thickness t. But

$$T = I/I_0 \tag{14}$$

or

$$T = \frac{r_1 - r_3}{r_0 - r_2} = e^{-n\,t\sigma} \tag{15}$$

The fractional error $\Delta\sigma/\sigma$ in the cross section σ is obtained by applying the law of propagation of error[8] to

$$\sigma = \frac{-\ ln\ T}{n\ t} \tag{16}$$

so that[9]

$$\left(\frac{\Delta\sigma}{\sigma}\right)^2 = \left(\frac{\partial\sigma}{\partial n}\ \frac{\Delta n}{\sigma}\right)^2 + \left(\frac{\partial\sigma}{\partial t}\ \frac{\Delta t}{\sigma}\right)^2 + \left(\frac{\partial\sigma}{\partial T}\ \frac{\Delta T}{\sigma}\right)^2 \tag{17}$$

The contribution of the third term alone need be considered since the product nt can be assumed known with negligible error. Subject to this condition we have

$$\left|\frac{\Delta\sigma}{\sigma}\right| = \left|\frac{\partial\sigma}{\partial T}\ \frac{\Delta T}{\sigma}\right| \tag{18}$$

---

[8] M. E. Rose and M. M. Shapiro, "Statistical Error in Absorption Experiments," ORNL-52, p. 6.

[9] *Ibid.*, p. 3.

using equation (16)

$$(19) \qquad \left(\frac{\Delta\sigma}{\sigma}\right)^2 = \left(\frac{\Delta T}{T \ ln \ T}\right)^2 = \left(\frac{\Delta T}{T} \ \frac{1}{n \ t \ \sigma}\right)^2$$

To evaluate $\Delta\sigma/\sigma$ we must first evaluate $\Delta T/T$. Applying the law of propagation of error to $\Delta T/T$ using (15)

$$(20) \qquad \frac{\Delta T}{T} = \frac{(\Delta r_1)^2 + (\Delta r_3)^2}{(r_1 - r_3)^2} + \frac{(\Delta r_0)^2 + (\Delta r_2)^2}{(r_0 - r_2)^2}$$

with $(\Delta c_i)^2 = c_i$, it follows from (8) that

$$(21) \qquad (\Delta r_i)^2 = \frac{r_i}{t_i} = \frac{c_i}{t_i^{\,2}}$$

Substituting from (9) and (21) into (20)

$$(22) \qquad \left(\frac{\Delta T}{T}\right)^2 = \frac{1}{(r_1 - r_3)^2}\left[\frac{c_1}{t_1^{\,2}} + \frac{c_1}{t_3^{\,2}} + T^2\left(\frac{c_0}{t_0^{\,2}} + \frac{c_2}{t_2^{\,2}}\right)\right]$$

Substituting (22) in (19)

$$(23) \qquad \left(\frac{\Delta\sigma}{\sigma}\right) = \frac{1}{(ln \ T)^2} \ \frac{1}{(r_1 - r_3)^2}\left[\frac{c_1}{t_1^{\,2}} + \frac{c_3}{t_3^{\,2}} + T^2\left(\frac{c_0}{t_0^{\,2}} + \frac{c_2}{t_2^{\,2}}\right)\right]$$

This formula has been used in computing the errors in σ indicated on the cross section graph, Figure 18 and Table IV.

CHAPTER III

INSTRUMENT PERFORMANCE

The bent crystal spectrometer used to obtain beams of nearly monochromatic neutron energy is an old X-ray crystal spectrometer which has been adapted for use with neutrons by L. Borst.[1] It is of the focusing type. Focusing at each energy is obtained by varying the crystal curvature.[2] The instrument has been overhauled quite thoroughly as part of the program of total neutron cross section measurements, to improve the Bragg reflected beam to background ratio and the handling ease. A photograph of the spectrometer is shown in Figure 3.

A schematic diagram of the neutron beam collimator, sample and spectrometer arrangement is shown in Figure 4. The sample is about four feet inside the pile shielding. The sample and counter are equidistant from the crystal.

For optimum focusing one should have a point source of neutrons. This is approximated by the use of a long graphite neutron collimator. At its origin deep in the pile, the beam is 3-3/8" × 3-3/8" square in cross sectional area. The collimator causes the beam to converge uniformly upon the sample. The beam is 3 millimeters in diameter when it emerges into the cavity of the graphite stringer section which contains the sample (Figures 4 and 5). Figure 6 shows the graphite stringer section with the sample containing assembly, which is known as the wafer, in place. The neutron beam is here defined by a Pyrex glass capillary tube, two inches in length and 1.5 millimeters inside diameter. The beam is then allowed to diverge as it leaves the sample. It emerges from the pile shielding and falls upon the bent crystal. Figure 4 shows how the sample is located at the common apex of the two cones of the collimator. Due to the small area of the beam at the position of the sample, the cross section of quite small amounts of material may be measured.

The procedure for measuring the transmission is to have two tubes, one carrying the sample, the other being empty. Readings are taken at a given energy with the sample in the beam and these are compared with readings taken with an identical empty tube in the beam. The sample shifter must be capable of removing one tube from the beam and placing the other in identically the same position.

---

[1] L. B. Borst, A. J. Ulrich, C. L. Osborne, and B. Hasbrouck, "Diffraction of Neutrons and Neutron Absorption Spectra," *The Physical Review*, 70:108, 1946.

[2] H. H. Johann, Zeitschr. *F. Physick*, 69:186, 1931.

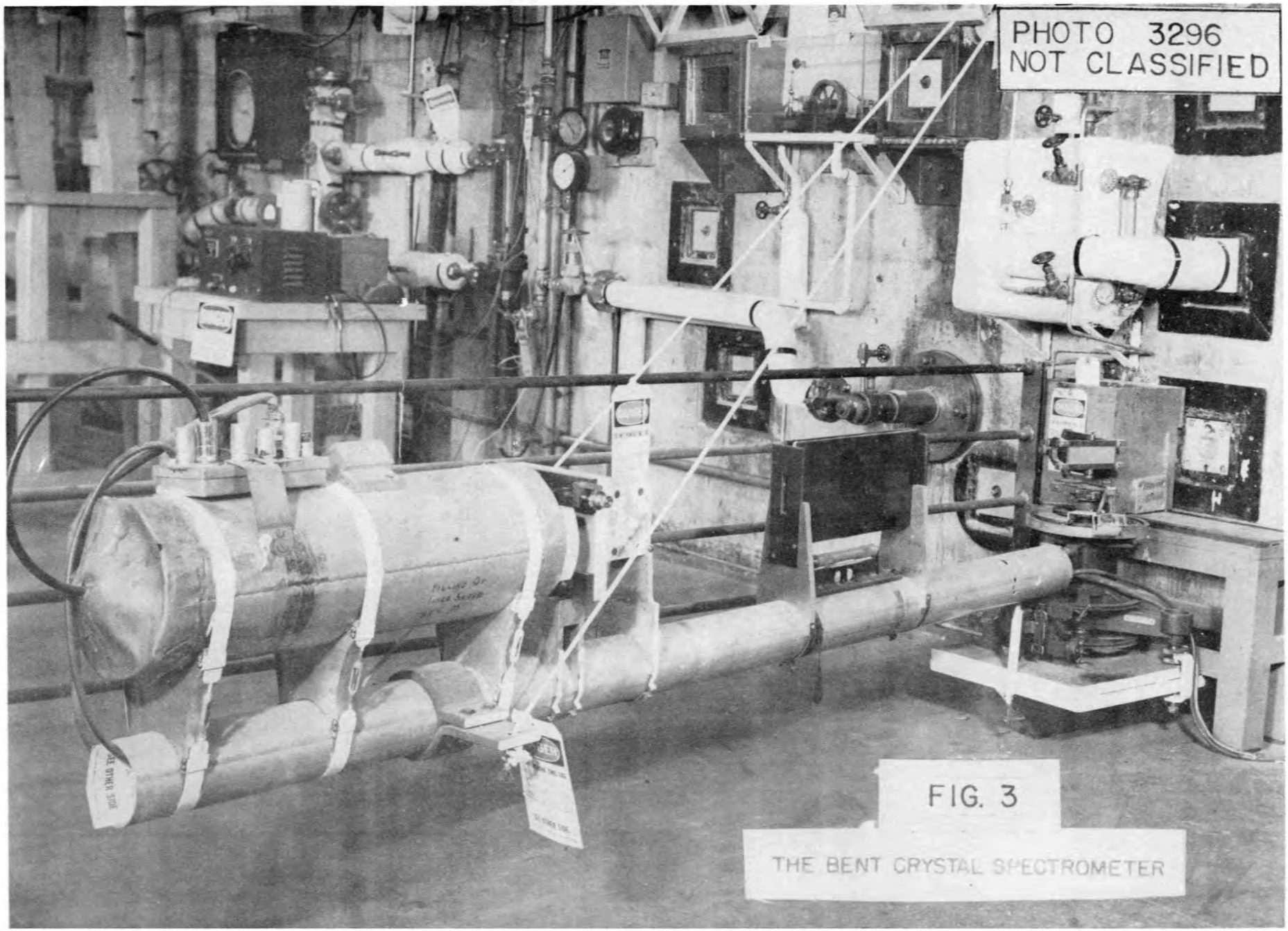

FIG. 3

THE BENT CRYSTAL SPECTROMETER

Dr. 6246
NOT CLASSIFIED

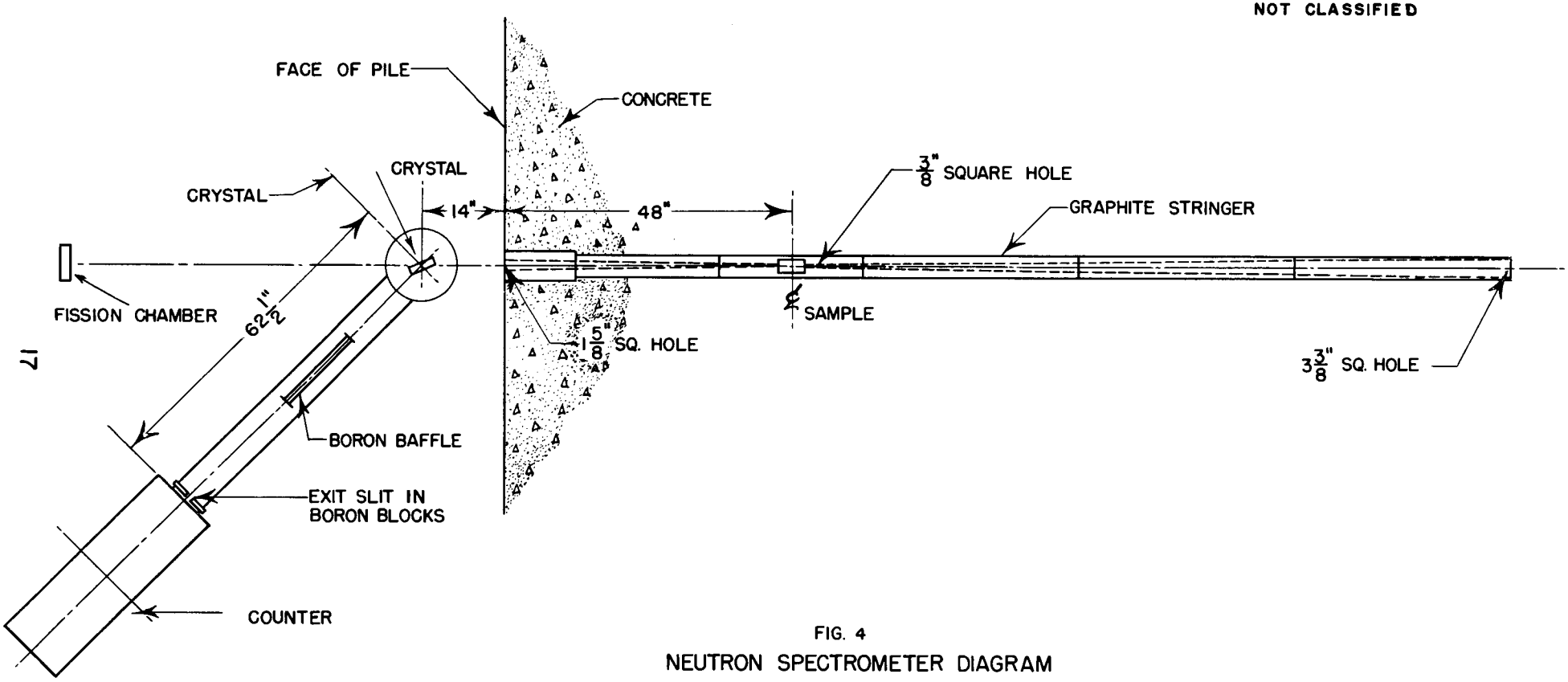

FIG. 4
NEUTRON SPECTROMETER DIAGRAM

1. REMOVABLE ROD TO OPERATE TOGGLE FOR POSITIONING SAMPLE SHIFTER AGAINST ADJUSTABLE STOP 4.
2. GROOVE FOR ELECTRICAL LEADS
3. ECCENTRIC SHAFT FOR LEVEL POSITIONING
4. ADJUSTABLE STOP
5. STATIONARY SHAFT
6. SAMPLE SHIFTER
7. GRAPHITE STRINGER
8. NEUTRON BEAM HOLE
9. CONNECTOR KEYWAY

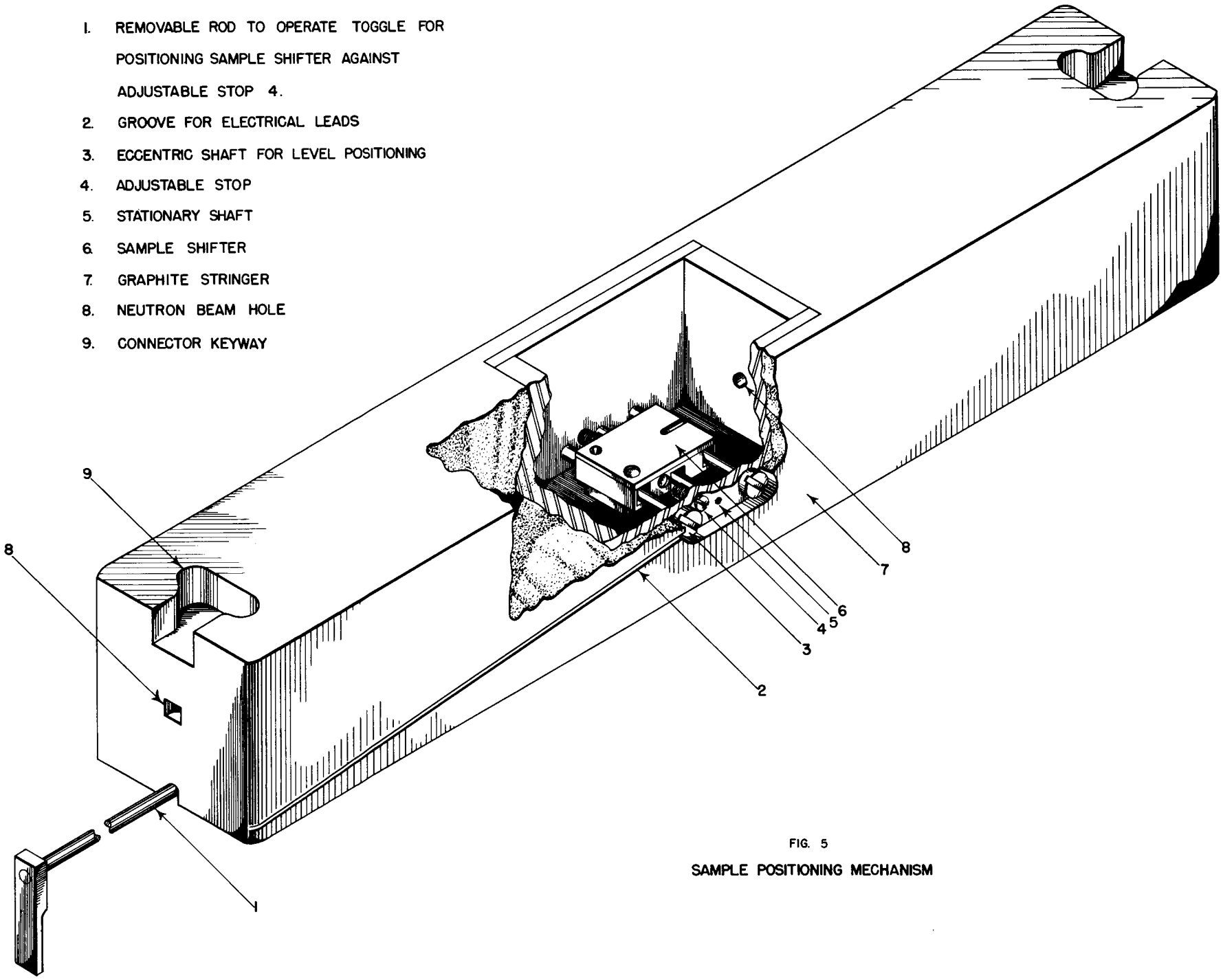

FIG. 5

SAMPLE POSITIONING MECHANISM

Dr. 6248
NOT CLASSIFIED

PHOTO 4413
NOT CLASSIFIED

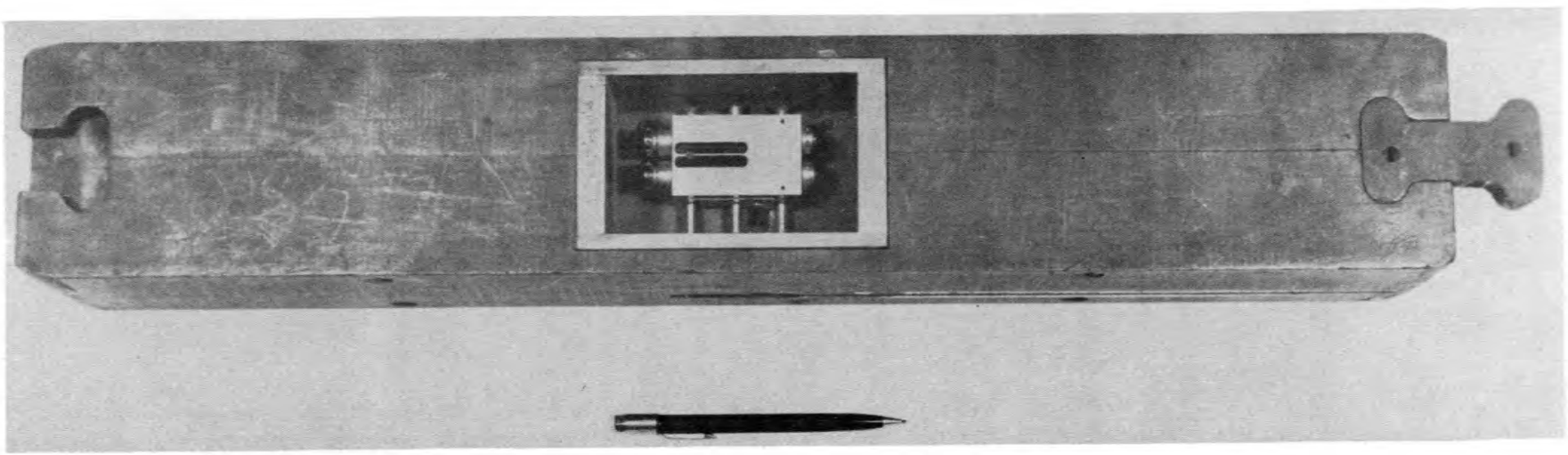

FIG. 6

SAMPLE SHIFTER SHOWING WAFER IN PLACE

The wafer consists of an aluminum block which holds two pieces of thick-walled precision-bore Pyrex capillary-tubing accurately parallel. An isometric drawing of the wafer is shown in Figure 7. For very accurate positioning the wafer is held by three eccentric hemispheres (see Figure 7) which seat themselves in the matching receptacles of the sample shifter, item 6 of Figure 5. The wafer is held in position by a permanent magnet in its base. Other adjustments for accurately placing the two capillaries in the neutron beam are in the sample shifter box shown in Figure 5. The sample tube and blank are interchanged by manipulating the lever (item 1 of Figure 5) which extends to the face of the pile.

The performance of the instrument is shown in the accompanying graphs. Figure 8 shows the counting rate as a function of neutron energy. A maximum counting rate of about 6000 counts per minute was obtained using a 2 millimeter capillary in the sample shifter and a 6 millimeter entrance slit to the counter. Figure 9 shows the background versus energy for the same conditions. The lower curve at the right is obtained by covering the counter entrance by thin foils of cadmium. Cadmium has a strong neutron resonance at 0.18 e.v. and continues to have a high cross section at lower energies due to the $1/v$ dependence of the absorption cross section.[3] Above 0.4 e.v., however, its cross section is quite small. For counting neutrons of greater than 0.4 e.v. a thin foil of cadmium is placed over the entrance slit. The cadmium removes a few of the beam neutrons but removes a large percentage of the slow neutrons of which the background is predominantly formed. Figure 10 shows the ratio of beam count to background where the improved ratio above 0.5 e.v. is again due to the use of cadmium foils.

Figure 11 shows how the counting rate varies as the crystal curvature is changed for a single energy. Focusing allows one to use a much narrower entrance to the counter, thus cutting the background down without sacrificing counting intensity. Figure 12, showing how the counting rate varies with counter entrance slit-width, gives an indication of the perfection of focusing. If the focus were perfect the maximum would be reached for 2 millimeters, the internal diameter of the capillary in the sample shifter.

---

[3] H. H. Goldsmith, "Neutron Cross Sections of the Elements," *Reviews of Modern Physics*, 19:282. 1947.

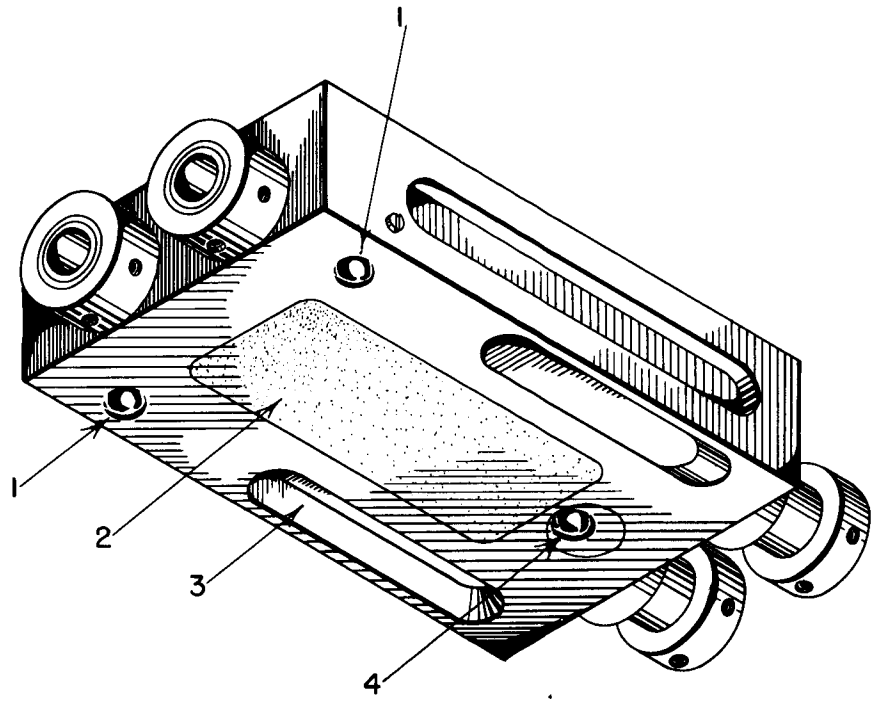

BOTTOM VIEW

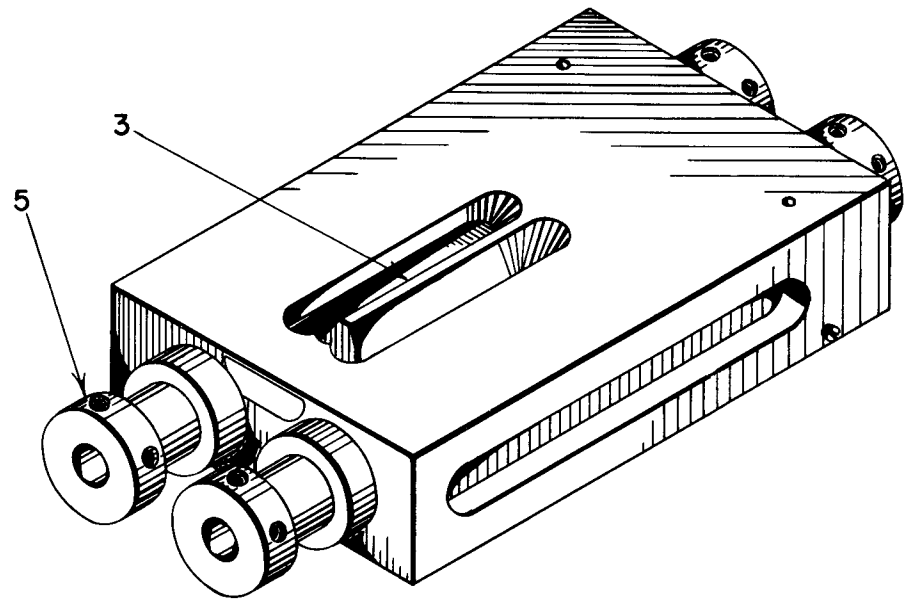

TOP VIEW

LEGEND

1. STATIONARY HALF-BALL
2. MAGNET - ALNICO - V
3. VIEWING SLOT
4. ECCENTRIC HALF - BALL
5. SAMPLE TUBE

FIG. 7
SAMPLE TUBE HOLDER

NOT CLASSIFIED

Dr 6264

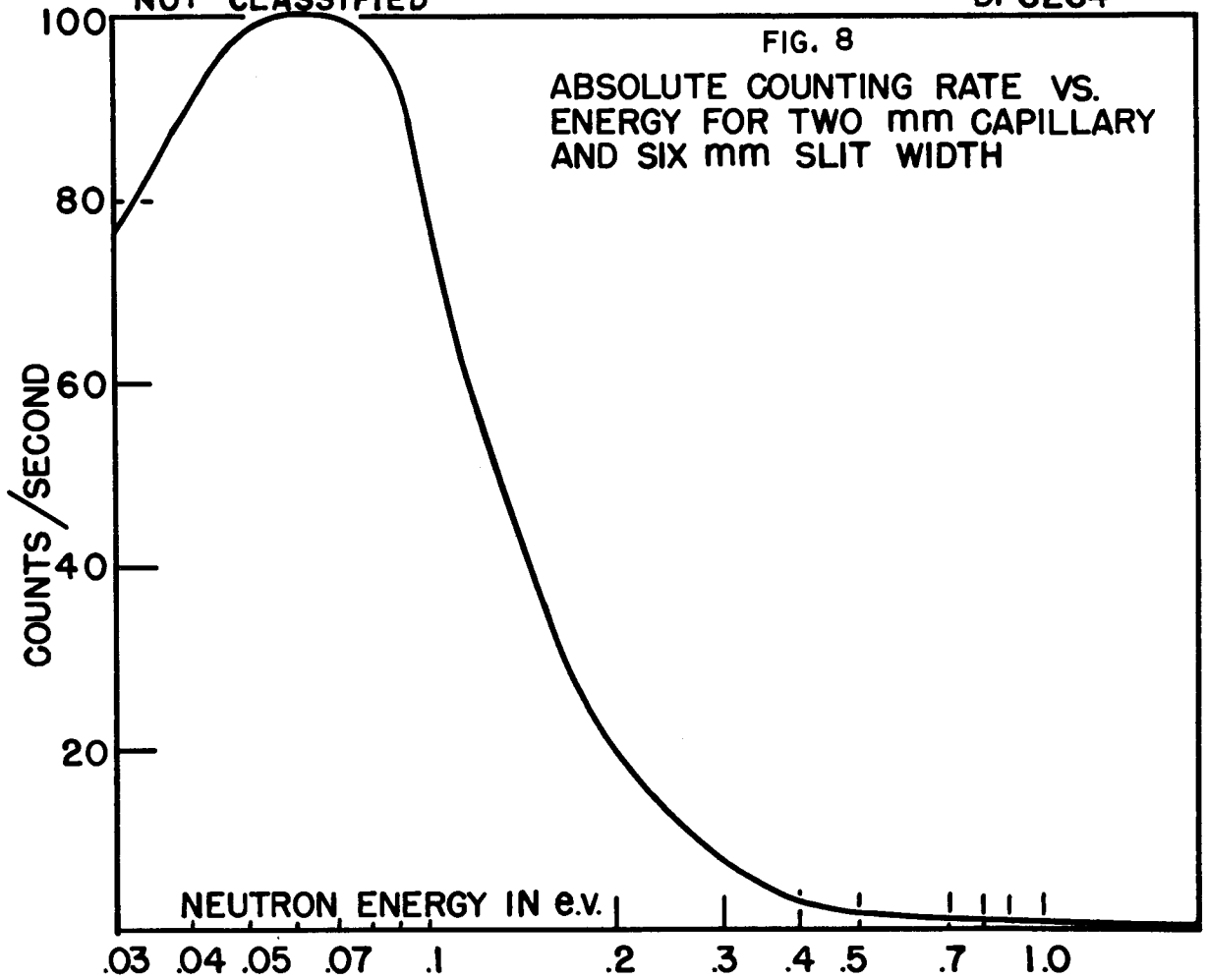

FIG. 8

ABSOLUTE COUNTING RATE VS. ENERGY FOR TWO mm CAPILLARY AND SIX mm SLIT WIDTH

NOT CLASSIFIED

Dr. 6265

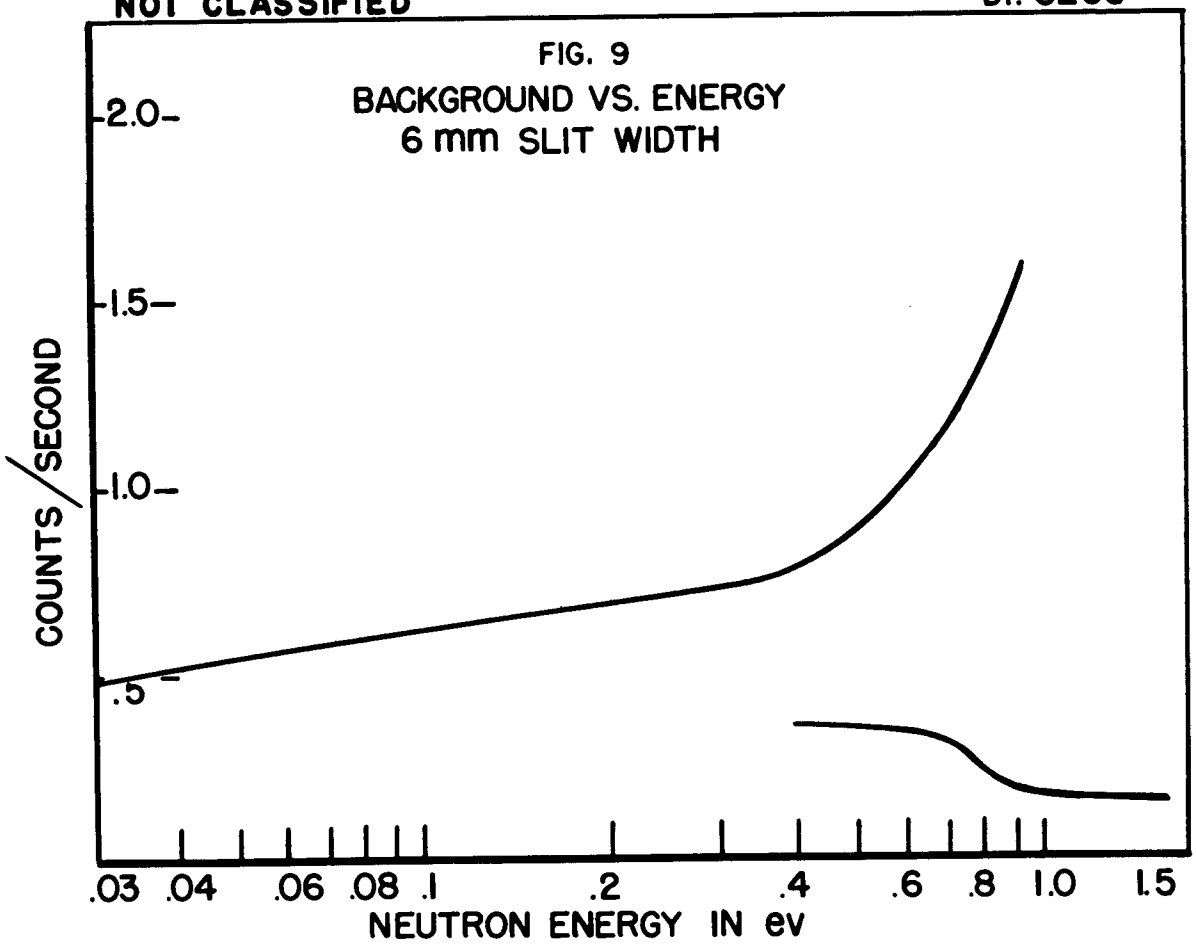

FIG. 9
BACKGROUND VS. ENERGY
6 mm SLIT WIDTH

NOT CLASSIFIED

Dr. 6266

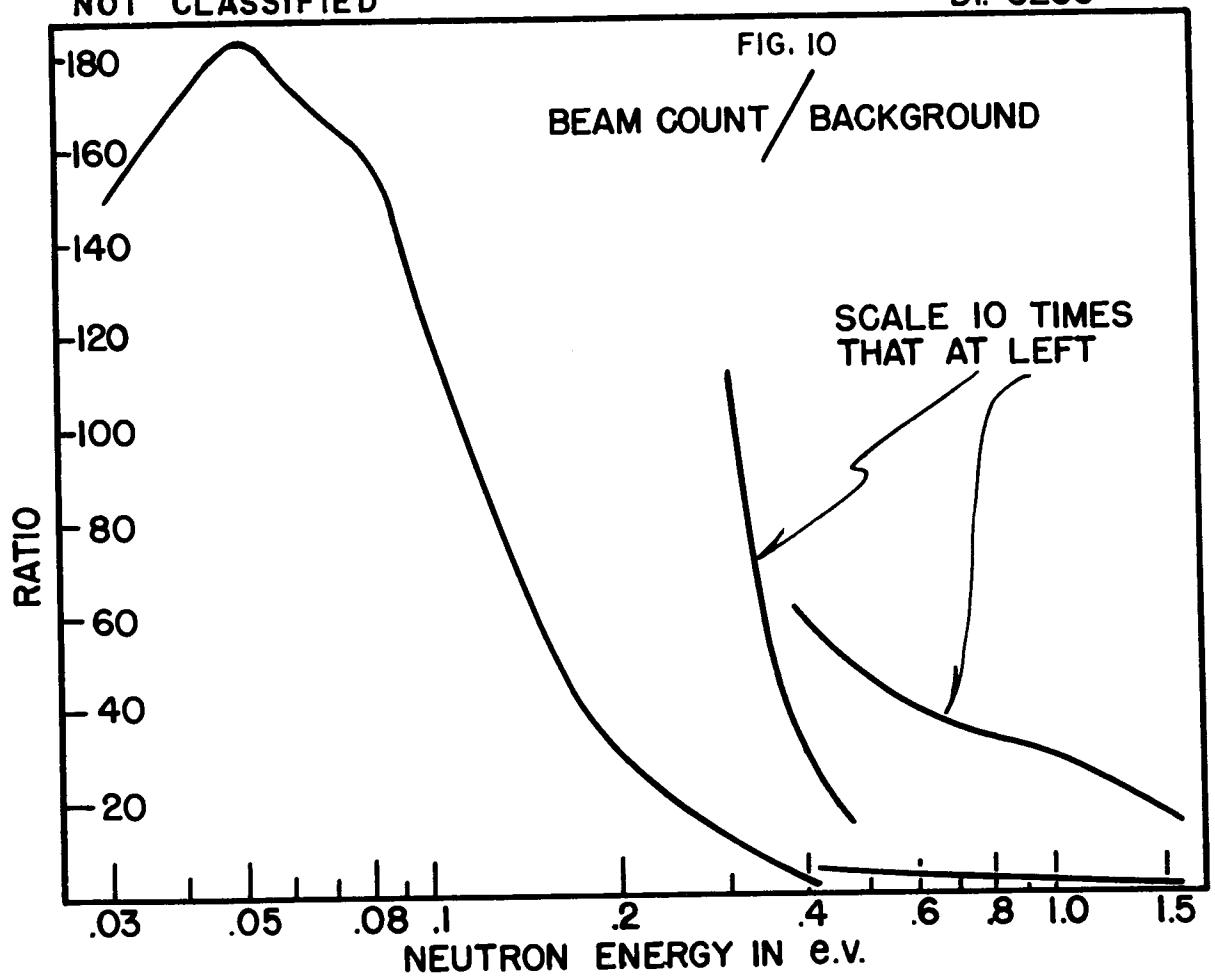

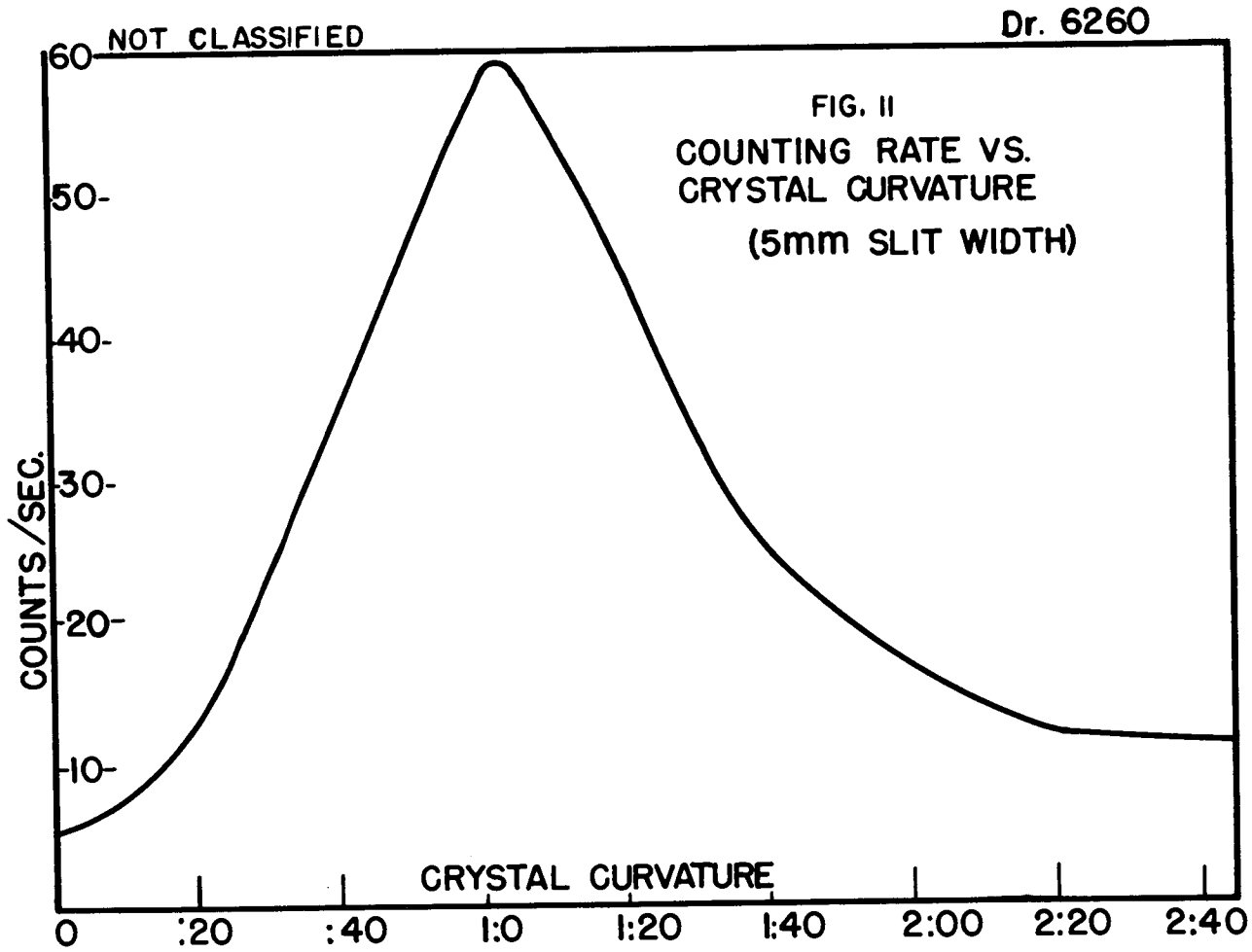
NOT CLASSIFIED
Dr. 6260
FIG. 11
COUNTING RATE VS.
CRYSTAL CURVATURE
(5mm SLIT WIDTH)
COUNTS/SEC.
60
50
40
30
20
10
CRYSTAL CURVATURE
0
:20
:40
1:0
1:20
1:40
2:00
2:20
2:40

NOT CLASSIFIED

Dr. 6259

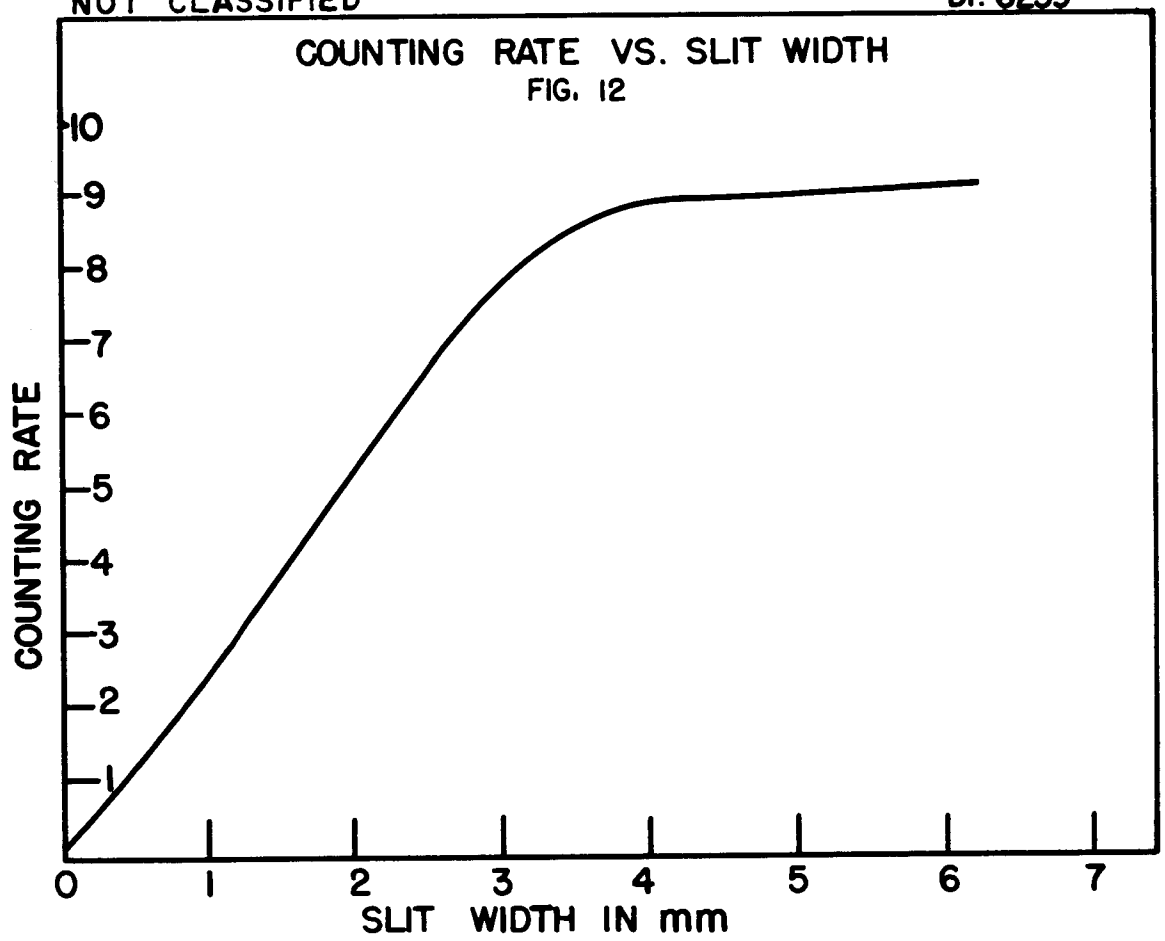

The sample shifter was tested in several ways. First the blank capillaries were aligned in the sample shifter box outside the pile, visually and with alignment jigs. The stringer section was then placed in position in the pile and the number of neutrons coming through each of the capillary tubes was measured with a fission chamber neutron detector in the direct beam. It was found that the number of counts coming through the two tubes could easily be made to agree within one per cent. The repositioning characteristics were next carefully checked by shifting repeatedly from one capillary tube to the other. The number of counts from each of the tubes remained constant within the statistical accuracy expected from the number of counts.

A much more severe test is to work with the beam reflected from the crystal to see if the ratio of the counts from the two capillaries is dependent on the setting of the crystal. If the capillaries were not parallel or if they did not occupy identical positions in the beam, this would show up in the rocking curve of one capillary being displaced with respect to the other. The term "rocking curve" refers to the curve of intensity vs. crystal angular setting for a fixed position of the detector. This rocking curve displacement test is very sensitive, due to the sharpness of the crystal rocking curve, and is important since one is unable to reset the spectrometer angle to better than one minute of arc with this instrument. The ratio of counts through the blank capillary to the count through the empty sample capillary must be reproducible. The actual rocking curves for the two tubes are shown in Figure 13, while Figure 14 shows the ratio of the counts in the reflected beam using one capillary tube, to the counts with the other capillary in place, as a function of crystal angle, the counter angle remaining fixed. The ratio remained constant for 4 minutes of crystal angle. The results of this test, with the other tests mentioned above indicated satisfactory performance of the sample shifter.

The Pyrex walls of the capillary actually define the neutron beam. Pyrex contains boron which has a neutron absorption cross section that varies inversely proportional to the neutron velocity. To test whether the length of path of the neutrons through the Pyrex walls was sufficient to define the neutron beam, a close fitting boron steel rod was inserted into the hole in one of the capillary tubes and the number of counts in the reflected beam measured from 0.3 e.v. to 0.5 e.v. This number was found to be indistinguishable from background within statistical accuracy.

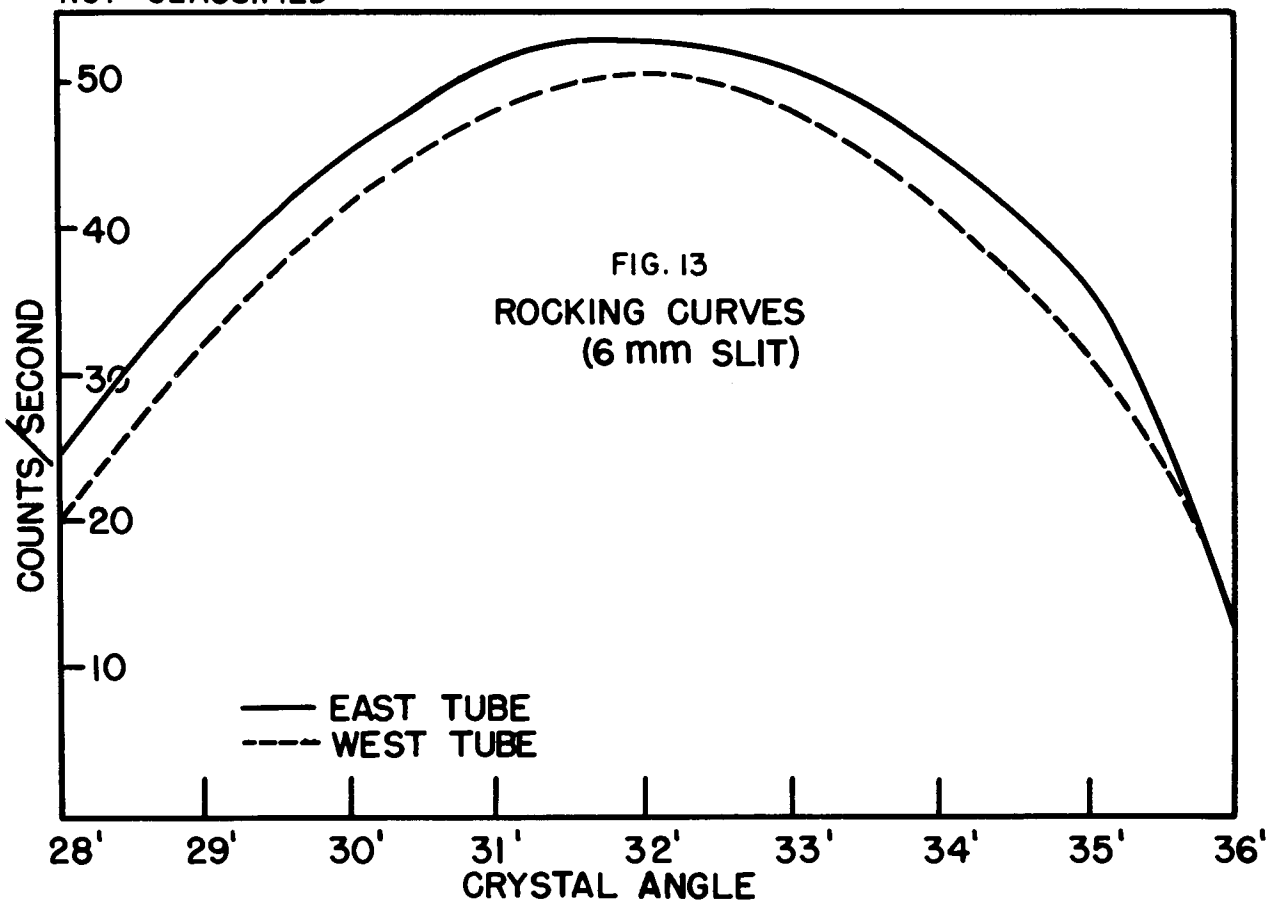

FIG. 13
ROCKING CURVES
(6 mm SLIT)

NOT CLASSIFIED

Dr. 6262

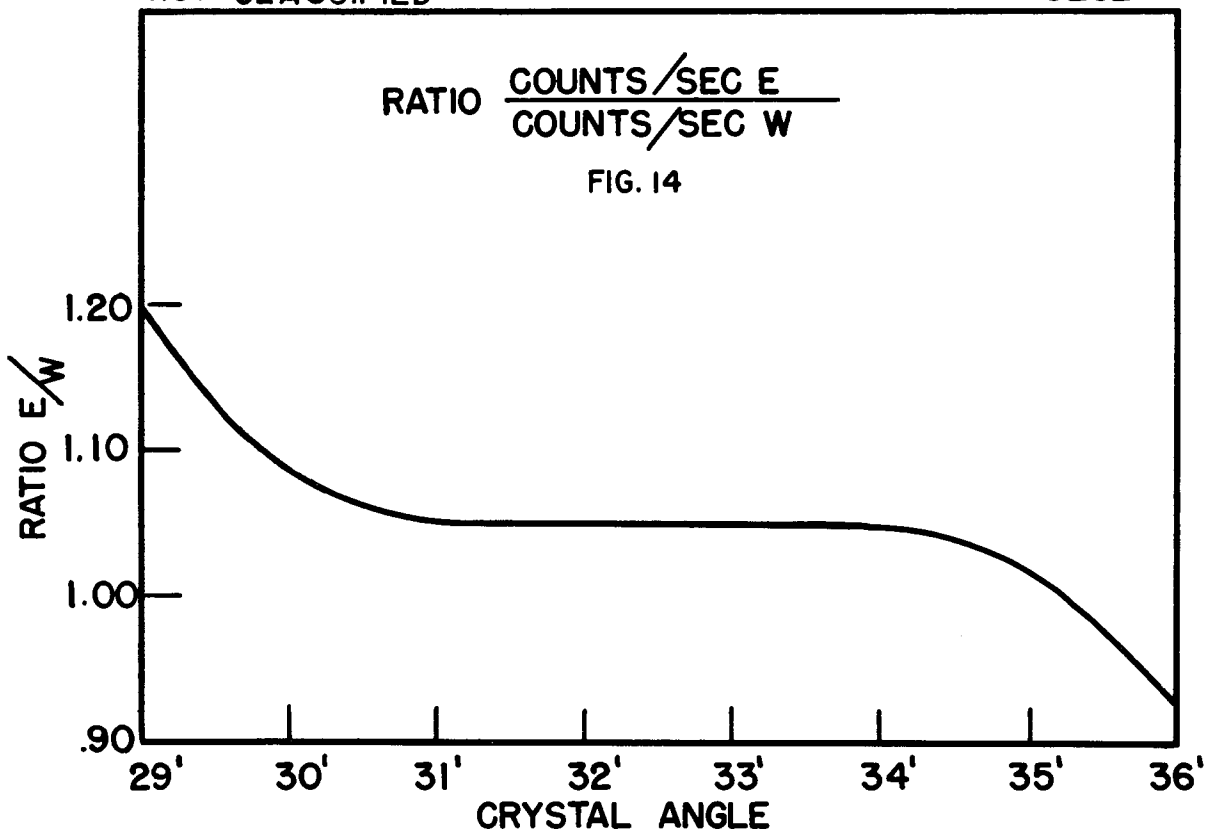

FIG. 14

In a test of the overall performance of the instrument the cross section of cadmium was measured over the small region of the peak of its resonance, from about 0.14 to 0.20 e.v. The results are shown in Figure 15. The peak value, 7300 barns, and general shape agree well with the published values.[4] These cadmium data constitute a test of the actual resolution of the instrument as well as a test for the sample shifter. Figure 15 shows the spectrometer is capable of detecting a 500 barn or 10 per cent change in cross section in a 0.01 e.v. interval at an energy of 0.15 e.v. The measurement of the cross section of $Ni^{58}O$ gives a more sensitive test of the instrument resolution. At 0.027 e.v. there is cross section discontinuity that was quite carefully investigated (See Figure 18). The obliquity of this step gives an indication of the resolution of the instrument since the line of discontinuity would be vertical for perfect resolution. The measured spread is 0.0006 e.v. which corresponds to an energy spread in the beam of plus or minus one per cent.

For a given θ the longest wave length λ that will satisfy the Bragg law

$$n \lambda = 2d \sin \theta$$

is obtained when $n = 1$, but for $n = 2$, $\lambda/2$, and for $n = 3$, $\lambda/3$, et cetera, also satisfy the Bragg law. Therefore, for a glancing angle and detector position appropriate to the energy E in the first order, the detector will receive, in addition to the energy E, the energy $4E$ (2nd order), $9E$ (3rd order), et cetera. At the higher energies there is a natural discrimination against the presence of higher orders by the flux distribution of the pile. The presence of higher order reflections from the quartz crystal was studied by transmission measurements of boron as a function of energy. When the results are plotted as in Figure 16, with the negative of the logarithm of the transmission times the square root of the neutron energy versus the energy, one gets a straight line parallel to the energy axis, in the absence of higher orders, since boron is a $1/v$ absorber. The falling off of the data from the horizontal line in Figure 16, at energies less than about 0.03 e.v., suggests the presence of higher order reflections in this region. The "falling off" is due simply to the fact that the addition of higher energy neutrons to the beam lowers the average cross

---

[4] Goldsmith, *loc. cit.*

NOT CLASSIFIED Dr. 6263

FIG. 15

CADMIUM CROSS SECTION VS. ENERGY
MEASURED BY TWO TUBE METHOD

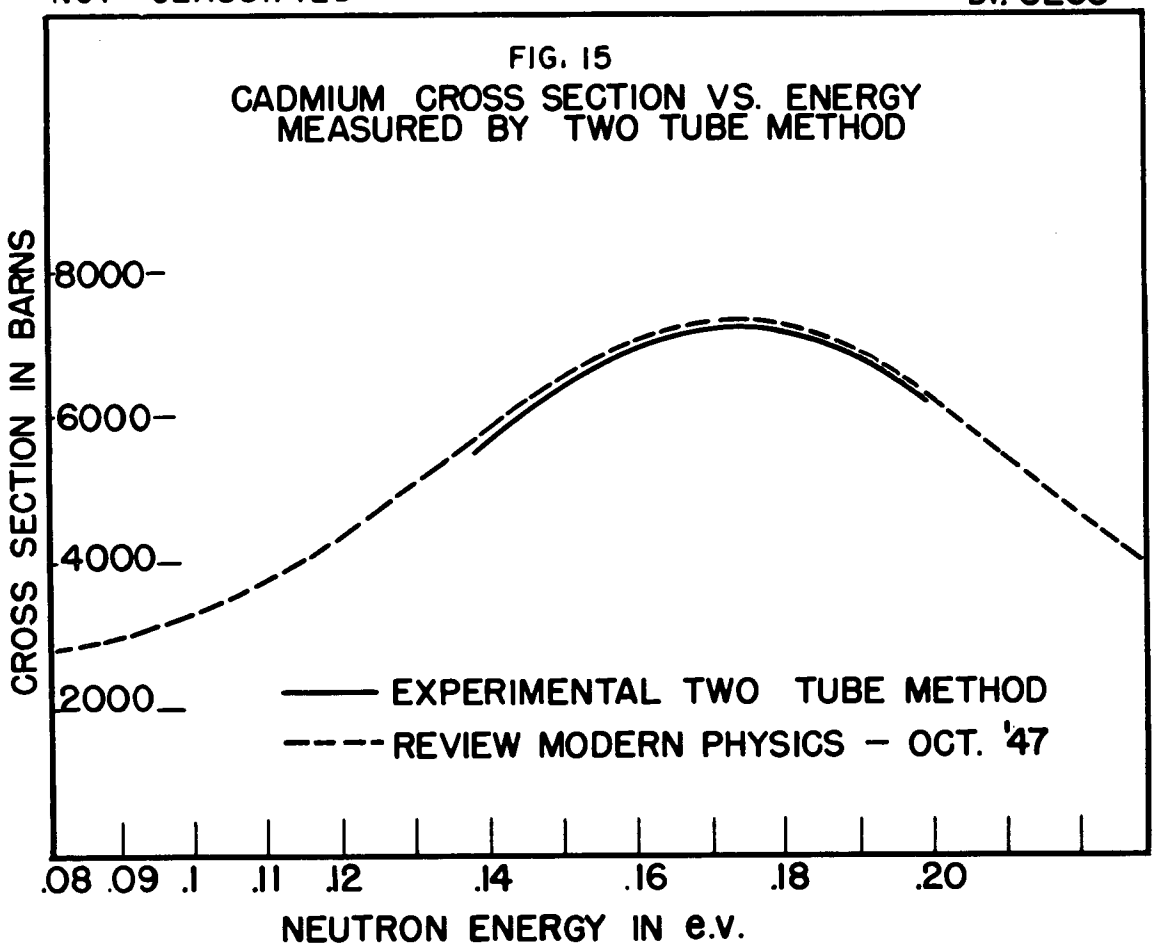

NOT CLASSIFIED

DWG. 4740

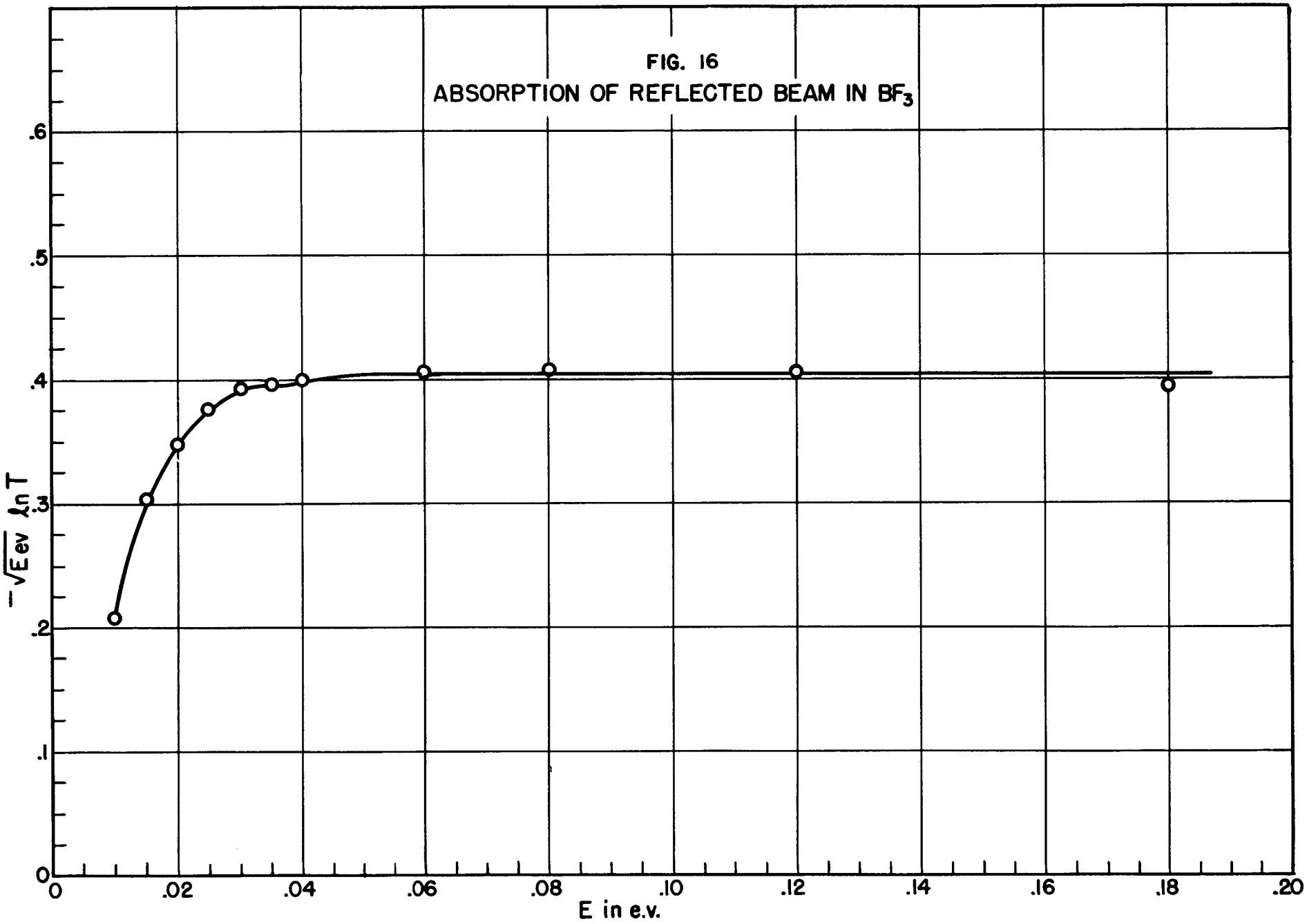

section of boron. In view of this information obtained from the boron measurements, no cross section measurements of Ni^{58} or Ni^{60} were taken at energies less than 0.025 e.v., where the number of higher order neutrons was considered to be appreciable.

The high energy limit of the instrument is set by decreasing beam intensity and increasing background. The peak of the flux distribution of the pile occurs below 0.1 e.v., and the number of neutrons of higher energy present decreases rapidly as the energy increases. The background increases with the setting for higher neutron energies, since higher energy means shorter wave length and smaller θ. Since the outside diameter of the counter shield is about 10 inches, the background could increase very markedly for scattering angles small enough for the direct beam to strike the counter shield. For this reason measurements were not taken at energies greater than 0.5 e.v.

The neutron detector is a boron trifluoride counter, the boron being enriched in the isotope B^{10}. It is the B^{10} isotope which is responsible for the neutron detection. Neutrons interact with B^{10} as follows:

$$ {}_5B^{10} + {}_0n^1 \longrightarrow {}_3Li^7 + {}_2\alpha^4 $$

The voltage on the anode is such that the charge of the original ionization produced by the liberated charged particles is multiplied many times during the time the charge is being collected. The pulse delivered to the grid of the first tube of the amplifier is proportional to the energy of the disintegration particles produced by the neutron for those disintegrations occurring so that both particles expend all of their energy in the gas of the chamber. The effective counter length is 18 inches. The outer shell is a 2 inch brass tube. The center wire (anode) diameter is 2 mils. The counter is filled to a pressure of 40 cm of mercury with BF_3. The operating voltage for the proportional counter is about 1800 volts. The ionization pulses were treated in the customary manner. They were first fed through a linear amplifier, then through a scaling circuit to a mechanical recorder. The electronic equipment used in shown schematically in Figure 17.

UNCLASSIFIED
DWG. 9348

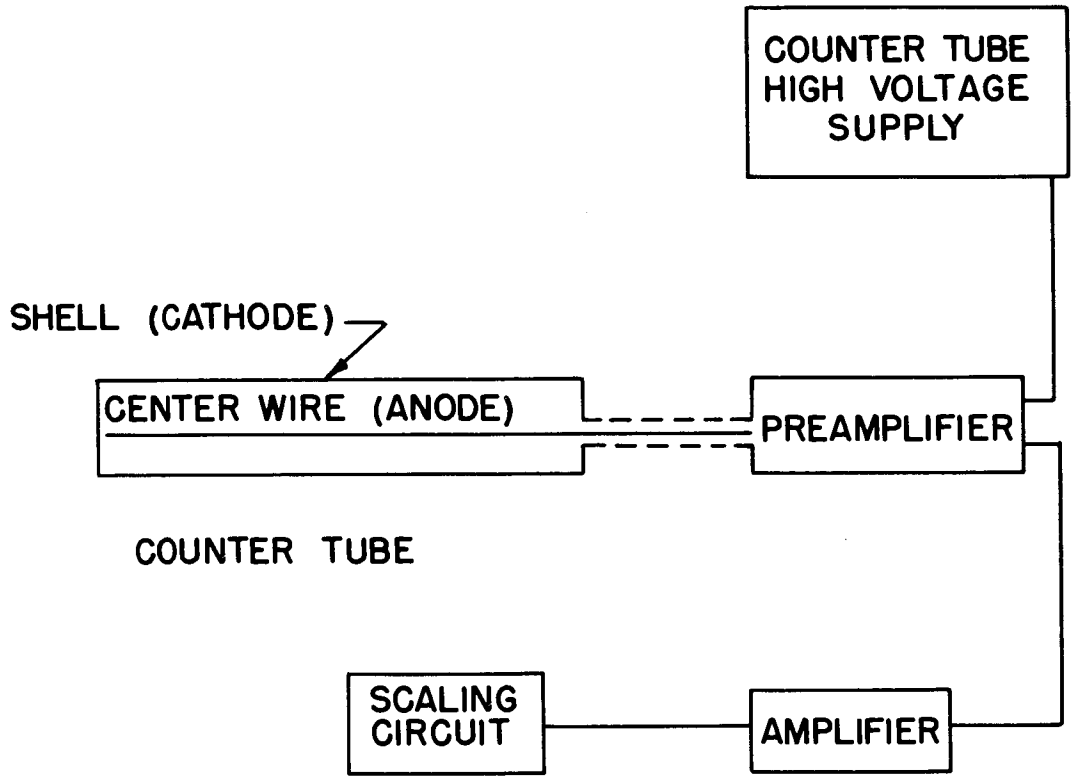

FIG. 17

SCHEMATIC CIRCUIT DIAGRAM

CHAPTER IV

EXPERIMENTAL DATA

The sample of Ni^{58} consisted of 0.1478 grams of NiO; the Ni^{60} sample consisted of 0.2189 grams of NiO. The samples were prepared by the Isotopes Production Division of the Electromagnetic Separation Plant at Oak Ridge, Tennessee. Their sample analysis is shown in Table I (normal Ni is shown for comparison). Mr. D. LaValle of the Oak Ridge National Laboratory Chemical Division furnished the water content analysis. The cross sectional area of the sample holding tube was 0.0314 cm^2, giving 4.705 grams per cm^2 for the Ni^{58} sample and 6.967 grams per cm^2 for the Ni^{60} sample.

The presence of undesired isotopes and water was corrected for by the use of the following equations:

(1)

$$T = e^{-(nt\sigma)_{Ni^{58}O}}\, e^{-(nt\sigma)_{Ni^{60}O}}\, e^{-(nt\sigma)_{Ni^{61}O}}\, e^{-(nt\sigma)_{Ni^{62}O}}\, e^{-(nt\sigma)_{H2O}}$$

(2)

$$-\ln T = (nt\sigma)_{Ni^{58}O} + (nt\sigma)_{Ni^{60}O} + (nt\sigma)_{Ni^{61}O} + (nt\sigma)_{Ni^{62}O} + (nt\sigma)_{H_2O}$$

The calculation of total cross section of $Ni^{58}O$ for the different neutron energies is shown in Table II. Column 1 lists the neutron energy. Column 2 gives the measured transmission. Column 3 is the transmission corrected for the difference in counts obtained through the empty sample capillary and the normal blank capillary. Column 5 corrects for the presence of nickel isotopes other than Ni^{58}. This is a small correction and a constant value of 5 barns, the calculated potential scattering cross section, was used for the total cross section of each nickel isotope. The cross section for oxygen was obtained from the *Reviews of Modern Physics*.[1]

The water content of the sample was only 1.1 per cent by weight, but this corresponds to about one-twentieth as many H_2O molecules as NiO. As water has a rather high slow neutron cross section which depends strongly on neutron

[1] H. H. Goldsmith, "Neutron Cross Sections of the Elements," *Reviews of Modern Physics*, 19:268, 1947.

TABLE I

Sample Analyses

	NORMAL Ni[a]	SAMPLE ENRICHED IN Ni^{58}	SAMPLE ENRICHED IN Ni^{60}
Ni^{58}	67.4%	98.1 %	1.9 %
Ni^{60}	26.7%	0.75%	97.7 %
Ni^{61}	1.2%	0.47%	0.2 %
Ni^{62}	3.8%	0.73%	0.1 %
Ni^{64}	0.9%	--	--
H_2O by Wt.	--	1.1 %	1.2 %
Other Impurities	--	--	Cu 0.04%

[a]*Handbook of Chemistry and Physics* (Cleveland, Ohio: Chemical Rubber Publishing Company, 1949), 31st Ed., p. 345.

TABLE II

Determination of Cross Section of $Ni^{58}0$ from Measured Transmission of Sample

(1)	(2)	(3)	(4)	(5)	(6)	(7)	(8)
				$nt\sigma$			
E, e.v.	T	T*	-ln T*	$Ni^{60}0$ $Ni^{61}0$ $Ni^{62}0$	H_20	$Ni^{58}0$	$\sigma Ni^{58}0$
0.0255	0.2610	0.2647	1.3292	0.0073	0.1695	1.1524	31.0
0.0265	0.2755	0.2794	1.2751	0.0073	0.1678	1.1000	29.6
0.0275	0.2791	0.2830	1.2719	0.0073	0.1661	1.0985	29.6
0.0280	0.2728	0.2766	1.2852	0.0073	0.1650	1.1129	29.9
0.0282	0.2541	0.2477	1.3560	0.0073	0.1647	1.1840	31.9
0.0285	0.2412	0.2446	1.4081	0.0073	0.1643	1.2365	33.3
0.0290	0.2462	0.2496	1.3879	0.0073	0.1633	1.2173	32.8
0.0295	0.2475	0.2510	1.3823	0.0073	0.1626	1.2124	32.6
0.0299	0.2523	0.2558	1.3634	0.0073	0.1616	1.1945	32.2
0.0305	0.2564	0.2600	1.3471	0.0073	0.1609	1.1935	32.1
0.0314	0.2664	0.2701	1.3090	0.0073	0.1595	1.1422	30.7
0.0324	0.2685	0.2723	1.3012	0.0073	0.1578	1.1361	30.6
0.0334	0.2712	0.2750	1.2910	0.0073	0.1564	1.1273	30.3
0.0353	0.2883	0.2923	1.2300	0.0073	0.1533	1.0694	28.8
0.0372	0.2993	0.3035	1.1924	0.0073	0.1515	1.0336	27.8
0.0384	0.2932	0.2973	1.2130	0.0072	0.1495	1.0563	28.4
0.0393	0.2930	0.2971	1.2137	0.0072	0.1488	1.0577	28.5
0.0412	0.3040	0.3083	1.1767	0.0072	0.1460	1.0235	27.6
0.0421	0.2947	0.2988	1.2080	0.0072	0.1446	1.0562	28.4
0.0431	0.2742	0.2780	1.2801	0.0072	0.1436	1.1293	30.4
0.0440	0.2907	0.2948	1.2215	0.0072	0.1429	1.0714	28.8
0.0451	0.2862	0.2902	1.2372	0.0072	0.1419	1.0881	29.3
0.0469	0.2875	0.2915	1.2327	0.0072	0.1398	1.0857	29.2
0.0489	0.2833	0.2873	1.2472	0.0071	0.1384	1.1017	29.7
0.0511	0.2929	0.2970	1.2140	0.0071	0.1367	1.0702	28.8
0.0523	0.2764	0.2803	1.2719	0.0071	0.1360	1.1288	30.4
0.0527	0.2800	0.2839	1.2591	0.0071	0.1349	1.1171	30.1
0.0538	0.2868	0.2908	1.2351	0.0071	0.1342	1.0938	29.4
0.0548	0.2928	0.2969	1.2144	0.0071	0.1339	1.0734	28.9
0.0569	0.2896	0.2937	1.2252	0.0071	0.1325	1.0856	29.2
0.0579	0.3019	0.3061	1.1838	0.0071	0.1318	1.0449	28.1
0.0587	0.2992	0.3034	1.1927	0.0071	0.1311	1.0545	28.4
0.0608	0.2941	0.2982	1.2100	0.0071	0.1304	1.0725	28.9
0.0627	0.3002	0.3044	1.1884	0.0071	0.1287	1.0526	28.3
0.0648	0.3004	0.3046	1.1888	0.0071	0.1273	1.0544	28.4
0.0663	0.2893	0.2934	1.2262	0.0071	0.1263	1.0928	29.4
0.0674	0.2831	0.2871	1.2480	0.0071	0.1259	1.1150	30.0

TABLE II

Determination of Cross Section of $Ni^{58}0$ from Measured Transmission of Sample (continued)

(1)	(2)	(3)	(4)	(5)	(6)	(7)	(8)
				$nt\sigma$			
E, e.v.	T	T*	-ln T*	$Ni^{60}0$ $Ni^{61}0$ $Ni^{62}0$	H_20	$Ni^{58}0$	σ $Ni^{58}0$
0.0686	0.2912	0.2953	1.2198	0.0071	0.1256	1.0871	29.3
0.0705	0.2918	0.2959	1.2177	0.0071	0.1242	1 0864	29.2
0.0722	0.2963	0.3004	1.2026	0.0071	0.1235	1.0720	28.9
0.0742	0.3056	0.3099	1.1715	0.0071	0.1225	1.0419	28.0
0.0763	0.3047	0.3090	1.1767	0.0071	0.1218	1.0478	28.2
0.0782	0.3067	0.3110	1.1680	0.0071	0.1211	1.0398	28.0
0.0805	0.3051	0.3094	1.1731	0.0071	0.1204	1.0456	28.1
0.0822	0.3036	0.3079	1.1780	0.0071	0.1197	1.0512	28.3
0.0845	0.3070	0 3113	1.1670	0.0071	0.1187	1.0412	28.0
0.0860	0.3034	0.3076	1.1790	0.0071	0.1176	1.0543	28.4
0.0880	0.2969	0.3011	1.2003	0.0071	0.1172	1.0760	29.0
0.0900	0.2983	0.3025	1.1957	0.0071	0.1166	1.0720	28.9
0.0919	0.2991	0.3033	1.1930	0.0071	0.1156	1.0703	28.8
0.0939	0.3040	0.3083	1.1767	0.0071	0.1152	1.0544	28.4
0.0958	0.3045	0.3088	1.1751	0.0071	0.1142	1.0538	28.4
0.0971	0.3004	0.3046	1.1888	0.0071	0.1138	1.0679	28.7
0.1025	0.2970	0.3012	1.2000	0.0071	0.1125	1.0804	29.1
0.1072	0.3032	0.3074	1.1796	0.0071	0.1107	1.0618	28.6
0.1122	0.3084	0.3127	1.1625	0.0070	0.1097	1.0458	28.2
0.1172	0.3107	0.3150	1.1552	0.0070	0.1083	1.0399	28.0
0.1263	0.3094	0.3137	1.1595	0.0070	0.1066	1.0457	28.1
0.1366	0.3075	0.3118	1.1654	0.0070	0.1040	1.0544	28.4
0.1466	0.3041	0.3084	1.1764	0.0070	0.1028	1.0666	28.7
0.1557	0.3135	0.3179	1.1460	0.0070	0.1007	1.0383	27.9
0.1753	0.3127	0.3171	1.1485	0.0070	0.0979	1.0436	28.1
0.1945	0.3108	0.3152	1.1545	0.0070	0.0952	1.0523	28.3
0.2231	0.3154	0.3198	1.1401	0.0070	0.0924	1.0407	28.0
0.2419	0.3112	0.3156	1.1533	0.0070	0.0910	1.0553	28.4
0.2645	0.3160	0.3204	1.1382	0.0070	0.0893	1.0419	28.0
0.2950	0.3187	0.3232	1.1295	0.0070	0.0879	1.0346	27.8
0.3394	0.3147	0.3191	1.1421	0.0070	0.0858	1.0493	28.2
0.3843	0.3188	0.3233	1.1292	0.0070	0.0841	1.0381	27.9
0.4906	0.3209	0.3254	1.1227	0.0070	0.0825	1.0332	27.8

energy, a constant average value for its cross section cannot be used. Its actual cross section at each energy must be used. The cross section values for H_2O were obtained from the *Reviews of Modern Physics*.[2] In order to correct for the water content of the sample, a 10 per cent correction was subtracted from the value of the cross section obtained by assuming that the sample was entirely $Ni^{58}O$. This correction is shown in columns 4 and 6. Column 7 gives $nt\,\sigma$ for $Ni^{58}O$, from which σ for $Ni^{58}O$ is obtained. The values of the total cross section of $Ni^{58}O$ are listed in column 8.

Crystal angles and the calculation of their corresponding neutron energies are shown in Table III. Equation 4, Chapter II was used:

$$E = \frac{1.136 \times 10^{-3}}{\sin^2 \theta}$$

Figure 18 shows the total cross section of $Ni^{58}O$ as a function of energy. Figure 19 shows the total cross section of $Ni^{60}O$. The Miller indices responsible for the various peaks are indicated at the appropriate energy values for $Ni^{58}O$. This correspondence is discussed below.

The use of Equation 23, Chapter II for the calculation of the statistical error is indicated in Table IV for a few typical energies. These errors are shown on Figure 18.

---

[2] *Ibid.*, p. 261.

TABLE III

Neutron Energy Determination from the Crystal Angle

CRYSTAL ANGLE	θ	$\sin\theta$	$\sin^2\theta$	E, e.v.
87°39′	12°10.5′	0.21090	0.04448	0.0255
87°53′	11°56.5′	0.2069	0.04282	0.0265
88°06′	11°43.5′	0.2031	0.04126	0.0275
88°12′	11°37.5′	0.2014	0.04055	0.0280
88°15′	11°34.5′	0.2007	0.04026	0.0282
88°18′	11°31.5′	0.1998	0.03992	0.0285
88°24′	11°25.5′	0.1981	0.03924	0.0290
88°31′	11°18.5′	0.1961	0.03845	0.0295
88°35′	11°14.5′	0.1951	0.03806	0.0299
88°40′	11°09.5′	0.1932	0.03734	0.0305
88°52′	10°57.5′	0.1902	0.03619	0.0314
89°02′	10°47.5′	0.1872	0.05506	0.0324
89°11′	10°38.5′	0.1845	0.03405	0.0334
89°29′	10°20.5′	0.1794	0.03217	0.0353
89°46′	10°03.5′	0.1747	0.03050	0.0372
89°55′	9°54.5′	0.1721	0.02961	0.0384
90°02′	9°47.5′	0.1701	0.02892	0.0393
90°16′	9°33.5′	0.1661	0.02758	0.0412
90°22′	9°27.5′	0.1642	0.02696	0.0421
90°29′	9°20.5′	0.1623	0.02638	0.0431
90°35′	9°14.5′	0.1606	0.02579	0.0440
90°41′	9°08.5′	0.1587	0.02520	0.0451
90°52′	8°57.5′	0.1557	0.02425	0.0469
91°04′	8°45.5′	0.1524	0.02323	0.0489
91°15′	8°34.5′	0.1491	0.02223	0.0511
91°20′	8°29.5′	0.1477	0.02174	0.0523
91°23′	8°26.5′	0.1468	0.02155	0.0527
91°28′	8°21.5′	0.1454	0.02113	0.0539
91°33′	8°16.5′	0.1439	0.02072	0.0548
91°42′	8°07.5′	0.1413	0.01998	0.0569
91°46′	8°03.5′	0.1400	0.01961	0.0579
91°49′	8°00.5′	0.1392	0.01937	0.0587
91°58′	7°51.5′	0.1367	0.01870	0.0608
92°06′	7°43.5′	0.1346	0.01811	0.0627
92°13′	7°36.5′	0.1324	0.01753	0.0648
92°18′	7°31.5′	0.1310	0.01715	0.0663
92°22′	7°27.5′	0.1298	0.01685	0.0674
92°27′	7°23.5′	0.1287	0.01655	0.0686

TABLE III

Neutron Energy Determination from the Crystal Angle (continued)

CRYSTAL ANGLE	θ	$\sin\theta$	$\sin^2\theta$	E e.v.
92°32′	7°17.5′	0.1269	0.01611	0.0705
92°37′	7°12.5′	0.1255	0.01574	0.0722
92°43′	7°06.5′	0.1237	0.01531	0.0742
92°49′	7°00.5′	0.1220	0.01489	0.0763
92°54′	6°55.5′	0.1206	0.01454	0.0782
93°00′	6°49.5′	0.1288	0.01412	0.0805
93°04′	6°45.5′	0.1175	0.01382	0.0822
93°10′	6°39.5′	0.1159	0.01344	0.0845
93°13′	6°36.5′	0.1149	0.01321	0.0860
93°18′	6°31.5′	0.1136	0.01291	0.0880
93°22′	6°27.5′	0.1123	0.01262	0.0900
93°26′	6°23.5′	0.1112	0.01236	0.0919
93°30′	6°19.5′	0.1100	0.01210	0.0939
93°34′	6°15.5′	0.1089	0.01185	0.0958
93°37′	6°12.5′	0.1081	0.01169	0.0871
93°47′	6°02.5′	0.1053	0.01108	0.1025
93°55′	5°54.5′	0.1029	0.01060	0.1072
94°03′	5°46.5′	0.1006	0.01012	0.1122
94°11′	5°38.5′	0.0985	0.00969	0.1172
94°23′	5°26.5′	0.0948	0.00899	0.1263
94°35′	5°14.5′	0.0912	0.00832	0.1366
94°47′	5°02.5′	0.0880	0.00775	0.1466
94°55′	4°54.5′	0.0854	0.00730	0.1557
95°12.5′	4°37 ′	0.0805	0.00648	0.1753
95°27′	4°22.5′	0.0764	0.00584	0.1945
95°44′	4°05.5′	0.0714	0.00509	0.2231
95°53′	3°56.5′	0.0686	0.00411	0.2419
96°04′	3°45.5′	0.0658	0.00430	0.2645
96°16′	3°33.5′	0.0621	0.00385	0.295
96°30.5′	3°19 ′	0.0579	0.00335	0.339
96°42.5′	3°07 ′	0.0544	0.00296	0.384
97°04′	2°45.5′	0.0481	0.00232	0.491

Dr 6151
NOT CLASSIFIED

FIG. 18

TOTAL CROSS SECTION OF $Ni^{58}O$

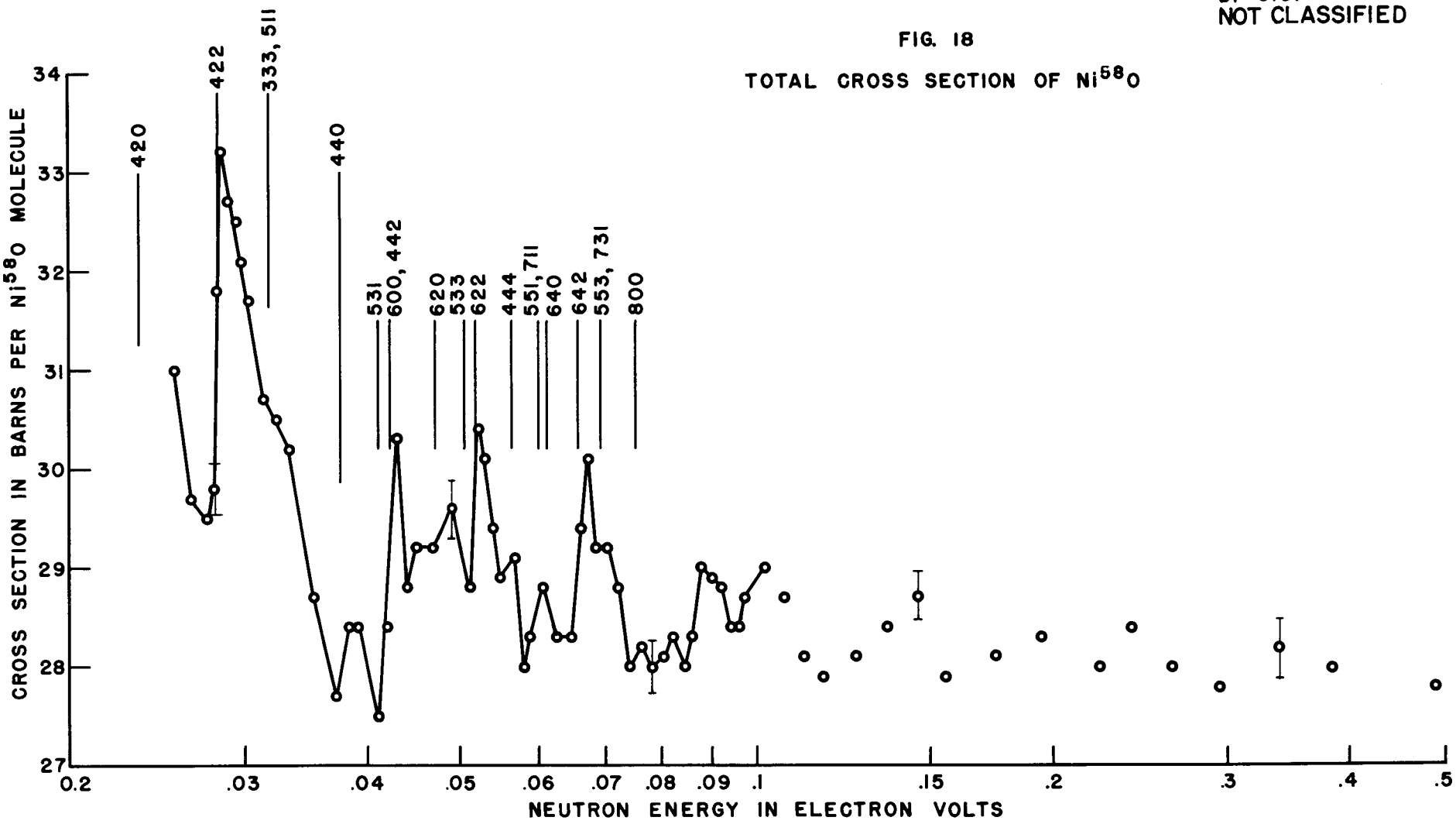

NOT CLASSIFIED

Dr 6423

FIG. 19

TOTAL CROSS SECTION OF $Ni^{60}O$
CORRECTED FOR WATER IMPURITY

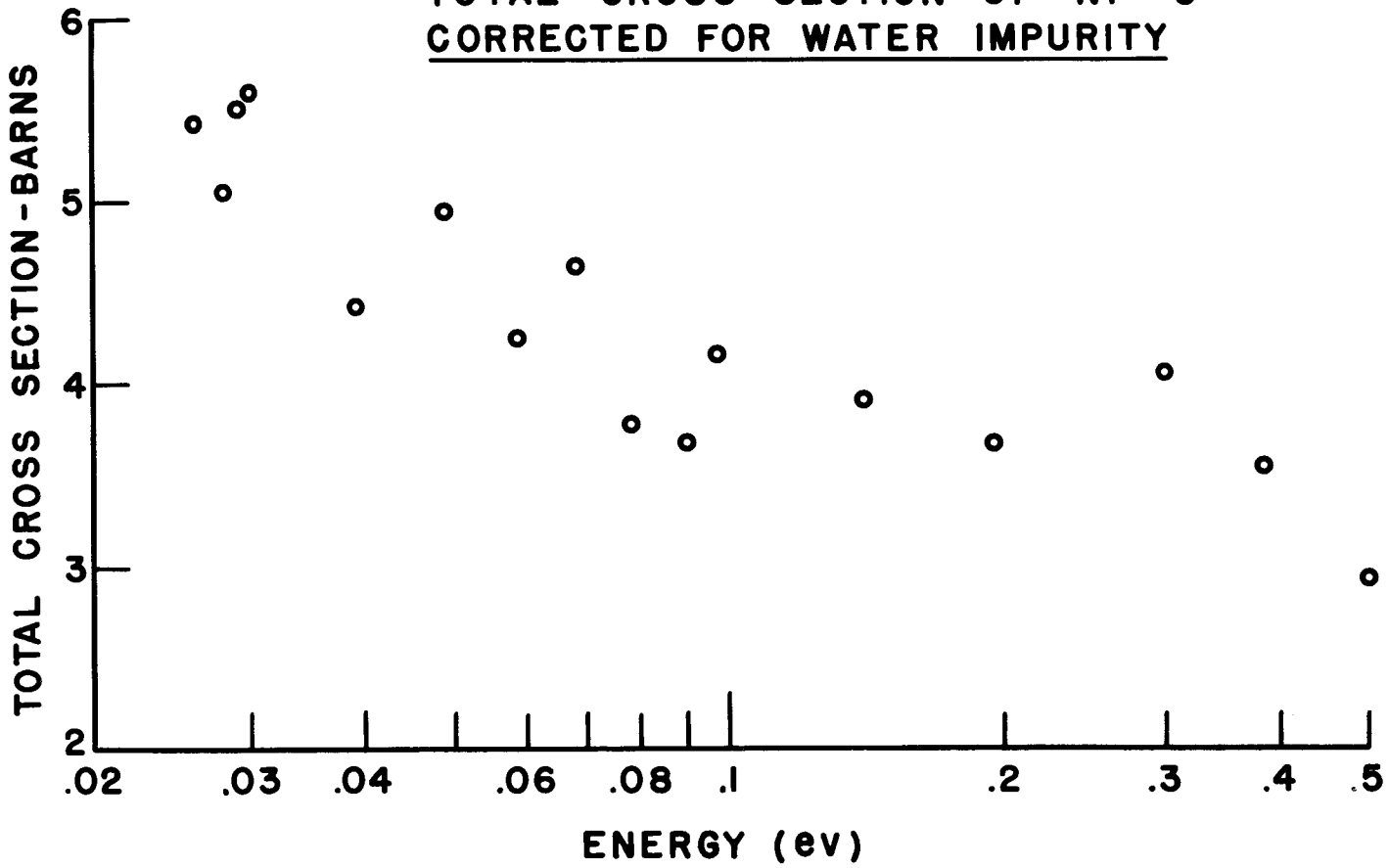

TABLE IV

Calculation of Statistical Error

	Energy				
	0.028 e.v.	0.0489 e.v.	0.0782 e.v.	0.1466 e.v.	0.0339 e.v.
(1) r_0	65.81	76.01	82.88	36.18	4.418
(2) r_1	18.60	26.63	25.31	11.91	1.628
(3) r_2	1.34	1.13	1.14	1.63	0.695
(4) r_3	0.98	0.94	0.87	1.19	0.467
(5) c_0	72,397	60,806	72,250	57,171	34,330
(6) c_1	59,725	47,962	65,312	32,755	18,221
(7) c_2	672	282	410	538	1,946
(8) c_3	538	320	346	595	2,746
(9) t_0	1,100	800	920	1,580	7,770
(10) t_1	3,210	1,801	2,580	2,750	11,193
(11) t_2	500	250	360	330	2,800
(12) t_3	550	340	400	500	5,880
(13) (2) - (4)	17.62	25.69	24.44	10.72	1.161
(14) $(13)^2$	310.5	660.0	597.3	114.92	1.348
(15) T	0.277	0.287	0.287	0.308	0.319
(16) T^2	0.0767	0.0824	0.0967	0.0949	0.1018
(17) -ln T	1.2852	1.2472	1.1680	1.1764	1.1421
(18) $(17)^2$	1.652	1.556	1.364	1.384	1.304
(19) $(5)/(9)^2 = (1)/(9)$	0.05983	0.09501	0.09008	0.02290	0.000569

TABLE IV (Cont'd)

	Energy				
	0.028 e.v.	0.0489 e.v.	0.0782 e.v.	0.1466 e.v.	0.339 e.v.
(20) $(6)/(10)^2 = (2)/(10)$	0.05794	0.14786	0.09810	0.00433	0.000145
(21) $(7)/(11)^2 = (3)/(11)$	0.00268	0.00452	0.00317	0.00494	0.000248
(22) $(8)/(12)^2 = (4)/(12)$	0.00178	0.00276	0.00218	0.00238	0.000079
(23) (19) + (21)	0.06251	0.09953	0.09325	0.02784	0.000817
(24) (16) (23)	0.00480	0.00820	0.009017	0.00264	0.0000832
(25) (20) + (22) + (24)	0.06452	0.15882	0.10930	0.00935	0.000307
(26) (18) (14)	512.9	1027.0	814.7	159.0	1.758
(27) 1/(26)	0.00195	0.000974	0.001227	0.006289	0.5688
(28) (25) (27)	0.000126	0.000155	0.000134	0.000059	0.000175
(29) $\sqrt{28} = \Delta\sigma/\sigma$	0.0112	0.0124	0.0116	0.0077	0.0132
(30) σ (barns)	29.9	29.7	28.0	28.7	28.2
(31) $\Delta\sigma$ = (29) σ (barns)	0.33	0.37	0.32	0.22	0.37

CHAPTER V

DISCUSSION OF EXPERIMENTAL RESULTS

NiO[1] like NaCl[2] has a face centered cubic structure. The distance between parallel planes for NiO is:[3]

$$d = \frac{a_2}{\sqrt{h^2 + k^2 + l^2}} \tag{1}$$

where a_0 = 4.172 A[4] and h, k, and l are the Miller indices. The equation for Bragg reflection from any parallel set of planes is:

$$n \lambda = 2d \sin \theta \tag{2}$$

The longest λ that can be reflected from this set of planes occurs when $\sin \theta = 1$ and $n = 1$, then

$$\lambda_m = 2d_{hkl} \tag{3}$$

Using Equation 7, Chapter II we obtain:

$$\lambda_m = 2d_{hkl} = \frac{0.286}{\sqrt{E_m \text{ in e.v.}}} \text{ angstrom units} \tag{4}$$

where E_m corresponds to the lowest energy that can be scattered from this set of planes.

For wave lengths greater than λ_m there will be no coherent scattering by the crystal for those planes satisfying the relation $\lambda_m = 2d_{hkl}$. For wave

---

[1] *Handbook of Chemistry and Physics* (Cleveland, Ohio: Chemical Rubber Publishing Company, 1949), 31st Ed., p. 2065.

[2] *Ibid.*, p. 2064.

[3] M. J. Buerger, *X-Ray Crystallography* (New York: John Wiley and Sons, 1942), p. 103.

[4] *Handbook of Chemistry and Physics, op. cit.*, p. 2065.

lengths less than λ_m, there will be coherent scattering which falls off monotonically with decreasing wave length. Consequently there will be a discontinuity in the curve of intensity versus energy at the energy corresponding to λ_m.

The crystal structure factor per molecule is:[5]

$$F = \Sigma \frac{f_n}{N} e^{2\pi i \ (hx_n + ky_n + lz_n)} \tag{5}$$

Where h, k, l are the Miller indices of the crystal plane, N is the number of molecules per unit cell, f_n is the coherent scattering amplitude of the nth atom and summation is over the atoms in a unit cell.

For NiO the location of the atoms may be described in units of a_0 as follows:

4 Ni atoms at	000	½½0	0½½	½0½
4 0 atoms at	½½½	½00	0½0	00½

Expanding Equation 5 in trigonometric terms gives for NiO:

$$F = \frac{f_{Ni}}{4}\left[1 + \cos\pi(h+k) + \cos\pi(k+l) + \cos\pi(h+l)\right] + \frac{f_0}{4}\left[\cos\pi(h+k+l) + \cos\pi h + \cos\pi k + \cos\pi l\right] \tag{6}$$

When h, k, l are all even we have,

$$F = f_{Ni} + f_0 \tag{7}$$

When h, k, l are all odd we have,

$$F = f_{Ni} - f_0 \tag{8}$$

When h, k, l are not all odd or all even we have,

$$F = 0 \tag{9}$$

---

[5] A. H. Compton and S. K. Allison, *X-Rays in Theory and Experiment* (New York: D. Van Nostrand Company, Inc., 1935), p. 353.

Therefore only those planes for which h, k, l are all even or all odd will give coherent scattering and produce a discontinuity. Table V shows the calculation of the cut off energy for the first several contributing sets of Miller indices.

The coherent crystalline scattering effects are very distinct for $Ni^{58}O$. The fact that such large crystalline effects persist at energy values as high as 0.1 e.v. for the Ni^{58} sample indicates at once that Ni^{58} is the isotope responsible for the anomalously high scattering cross section noted by Koehler, Wollan and Shull.[6] The potential scattering cross section due to the physical size of the Ni nucleus is much less than the observed value of the scattering cross section.

Potential scattering $= 4 \pi R^2$ [7]

$R = 6.5 \times 10^{-13}$ cm = Nuclear radius of Ni.[8]

$4 \pi R^2 = 5.3$ barns

From the height of the cross section discontinuities, the scattering cross section of an individual bound nucleus may be calculated. Halpern, Hamermesh and Johnson[9] have developed the general theory of the scattering of neutrons on passage through crystalline materials. The following relationship, which is consistent with their results, is directly applicable to calculation of the coherent scattering cross section from the data of this experiment.

$$\frac{\sigma_{hkl}}{\text{molecule}} = \frac{\lambda^2 M}{2} j_{hkl} \, d_{hkl} \, F^2_{hkl} \, e^{-2W_{hkl}} \tag{10}$$

σ_{hkl} is the measured discontinuity in the cross section curve

λ is the wave length at which this discontinuity occurs

M is the number of molecules per cm^3

j_{hkl} is the multiplicity value for the particular reflection

---

[6] W. C. Koehler, E. O. Wollan and C. G. Shull, "The Coherent Scattering Cross Section of Nickel and Its Isotopes," *The Physical Review*, In press.

[7] H. Feshbach, D. C. Peaslie, and V. F. Weisskopf, "On the Scattering and Absorption of Particles by Atomic Nuclei," *The Physical Review*, 71: 145, 1947.

[8] E. Amaldi and B. N. Cacciapuoti, "On the Dependence of Nuclear Radius on the Mass Number," *The Physical Review*, 71:739, 1947.

[9] O. Halpern, M. Hamermesh, and M. H. Johnson, "The Passage of Neutrons Through Crystals and Polycrystals," *The Physical Review*, 59:981, 1941.

TABLE V

Energy Location of Crystalline Scattering Cross Section Discontinuities for NiO

MILLER INDICES h k l	$h^2 + k^2 + l^2$	$\sqrt{h^2 + k^2 + l^2}$	$d = \frac{4.172}{\sqrt{h^2 + k^2 + l^2}}$	$\lambda = 2d$	λ^2	$E = \frac{.08185}{\lambda^2}$
111	3	1.7321	2.408	4.817	23.216	0.0035
200	4	2.0000	2.086	4.172	17.406	0.0047
220	8	2.8284	1.475	2.950	8.703	0.0094
311	11	3.3166	1.258	2.516	6.329	0.0129
222	12	3.4641	1.204	2.409	5.802	0.0141
400	16	4.0000	1.043	2.086	4.351	0.0188
331	19	4.3589	0.957	1.914	3.664	0.0223
420	20	4.4721	0.933	1.866	3.481	0.0235
422	24	4.8990	0.851	1.703	2.901	0.0282
333,511	27	5.1961	0.803	1.606	2.579	0.0317
440	32	5.6569	0.737	1.475	2.176	0.0376
531	35	5.9161	0.705	1.410	1.989	0.0412
600,442	36	6.0000	0.695	1.391	1.934	0.0423
620	40	6.3246	0.659	1.319	1.741	0.0470
533	43	6.5574	0.636	1.273	1.619	0.0506
622	44	6.6333	0.629	1.258	1.582	0.0517
444	48	6.9282	0.602	1.204	1.451	0.0564
551,711	51	7.1414	0.584	1.168	1.365	0.0600
640	52	7.2111	0.578	1.157	1.339	0.0611

TABLE V (Cont'd)

MILLER INDICES h k l	$h^2 + k^2 + l^2$	$\sqrt{h^2 + k^2 + l^2}$	$d = \frac{4.172}{\sqrt{h^2 + k^2 + l^2}}$	$\lambda = 2d$	λ^2	$E = \frac{08185}{\lambda^2}$
642	56	7.4833	0.557	1.115	1.243	0.0658
553, 731	59	7.6811	0.543	1.086	1.180	0.0694
800	64	8.0000	0.521	1.043	1.088	0.0752
733	67	8.1854	0.509	1.019	1.039	0.0788
644, 820	68	8.2462	0.506	1.012	1.024	0.0799
660, 822	72	8.4853	0.491	0.983	0.967	0.0847
555,751	75	8.6603	0.481	0.963	0.928	0.0882
662	76	8.7178	0.478	0.957	0.916	0.0894
840	80	8.9443	0.466	0.933	0.870	0.0941
753, 911	83	9.1104	0.458	0.916	0.839	0.0976
842	84	9.1652	0.450	0.910	0.829	0.0988
664	88	9.3808	0.444	0.889	0.791	0.1035
931	91	9.5394	0.437	0.875	0.765	0.1083
844	96	9.7980	0.426	0.852	0.725	0.1129
755, 933	99	9.9499	0.419	0.839	0.703	0.1164
860, 100	100	10.0000	0.417	0.834	0.696	0.1176

d_{hkl} is the interplaner spacing for this set of planes

$F_{hkl} = f_{Ni} + f_0$ (h, k, l all even) where f_{Ni} and f_0 are the coherent scattering amplitudes for the bound Ni and O nuclei (See Equations 7 and 8).

$\sigma = 4 \pi f^2$

$e^{-2W_{hkl}}$ is a temperature correction factor with:[10]

$$W_{hkl} = \frac{6h^2}{mk\Theta}\left[\frac{\phi(x)}{(x)} + \frac{1}{4}\right]\frac{\sin^2\theta}{\lambda^2}, \quad x = \frac{\Theta}{T} \tag{11}$$

where h is Planck's constant, m is the average mass per atom of the molecule, k is Boltzmann's Constant, Θ is the Debye characteristic temperature $\phi(x)$ is the Debye function, λ is the neutron wave length and θ is the Bragg angle of reflection in the sample.

Since the atoms and hence the nuclei are in thermal agitation in the crystal, the effective coherent scattering amplitude will be somewhat smaller than the true nuclear amplitude. This is corrected for by the use of the Debye-Waller temperature correction factor W, so that[11]

$$f_T = f_0 \, e^{-W} \tag{12}$$

For the 422 discontinuity in NiO:

σ as measured from Figure 18 is 5.2×10^{-24} cm^2

$\lambda = 1.703 \times 10^{-8}$ cm

$M = 5.504 \times 10^{22}$

$j_{422} = 24$

$d_{422} = 0.851 \times 10^{-8}$

---

[10]Compton and Allison, *op. cit.*, p. 438.

[11]Compton and Allison, *loc. cit.*

The scattering cross section per free nucleus of oxygen is 3.73 barns.[12] The cross section for scattering by a rigidly bound nucleus will be greater than for the same nucleus in a free state by the square of the ratio of the neutron mass, to the reduced mass for the system, neutron plus scattering nucleus, *i.e.*

$$\frac{\sigma \text{ bound}}{\sigma \text{ free}} = \left[\frac{A + 1}{A}\right]^2. \tag{13}$$

Therefore σ_0 bound $= 4.21 \times 10^{-24}$ cm^2 giving

$f_0 = 0.58 \times 10^{-12}$ cm

f_{Ni} is to be determined

$\Theta = 500°K$ (an average value for this type substance)[13]

$T = 300°K$

$\Theta = 90°$

$x = 1.667$

$\phi(x) = 0.658$[14]

$m = 37 \times 1.6603 \times 10^{-24}$ g

Whence $W_{422} = 0.138$

$e^{-2W} = 0.76$

Using all of the above data and solving Equation 10 for the numerical value of F^2, the result is:

$$F^2 = 4.20 \times 10^{-24} \text{ cm}^2$$

---

[12] E. Melkonian, "Slow Neutron Velocity Spectrometer Studies of O_2, N_2, A, H_2, H_2O and Seven Hydrocarbons," *The Physical Review*, 76:1750, 1949.

[13] Compton and Allison, *op. cit.*, p. 438.

[14] *Ibid.*, p. 437.

From the expression for F^2_{hkl} for the 422 planes,

$$F^2 = (f_{Ni} - f_0)^2$$

the value $f_{Ni} = 1.47 \times 10^{-12}$ cm is calculated. This value for the coherent scattering amplitude of Ni^{58} corresponds to a coherent scattering cross section, $\sigma_{coh} = 27$ barns.

The peaks corresponding to sets of planes other than 422 could be used also to calculate f_{Ni}. However the results of such calculations would be far less accurate than for 422 because the magnitude of the discontinuity is so much smaller.

The value 27 barns for the coherent scattering cross section of the bound Ni^{58} nucleus corresponds to a scattering cross section for the free nucleus of about 26 barns. This value compares with the value of 24.5 barns obtained by using the average value of 28.2 barns given by the data in the region from 0.2 to 0.5 e.v., where crystalline and molecular binding effects should be small, and subtracting from it the value of 3.73 barns obtained by Melkonian for the free oxygen nucleus.

As $F_{hkl} = f_{Ni} + f_0$ for even h, k and l and $F_{hkl} = f_{Ni} = f_0$ for odd h, k and l (Equations 7 and 8), the fact that the 422 discontinuity is much larger than the 333, 511 discontinuity shows that Ni^{58} scatters with the same phase as does oxygen. This phase has arbitrarily been defined as positive by Fermi and Marshall.[15]

Feshbach, Peaslie and Weisskopf[16] calculated the effect of a scattering resonance on the scattering cross section. A plot of the scattering resonance giving the phase of scattering in the various energy regions is shown in Figure 20.

The magnitude of the scattering cross section compared to the value for potential scattering and the sign of the phase change on scattering permit speculation about the energy position of a possible scattering resonance.

---

[15] E. Fermi and L. Marshall, "Interference Phenomena of Slow Neutrons," *The Physical Review*, 71:666, 1947.

[16] Feshbach, Peaslie, and Weisskopf, *loc. cit.*

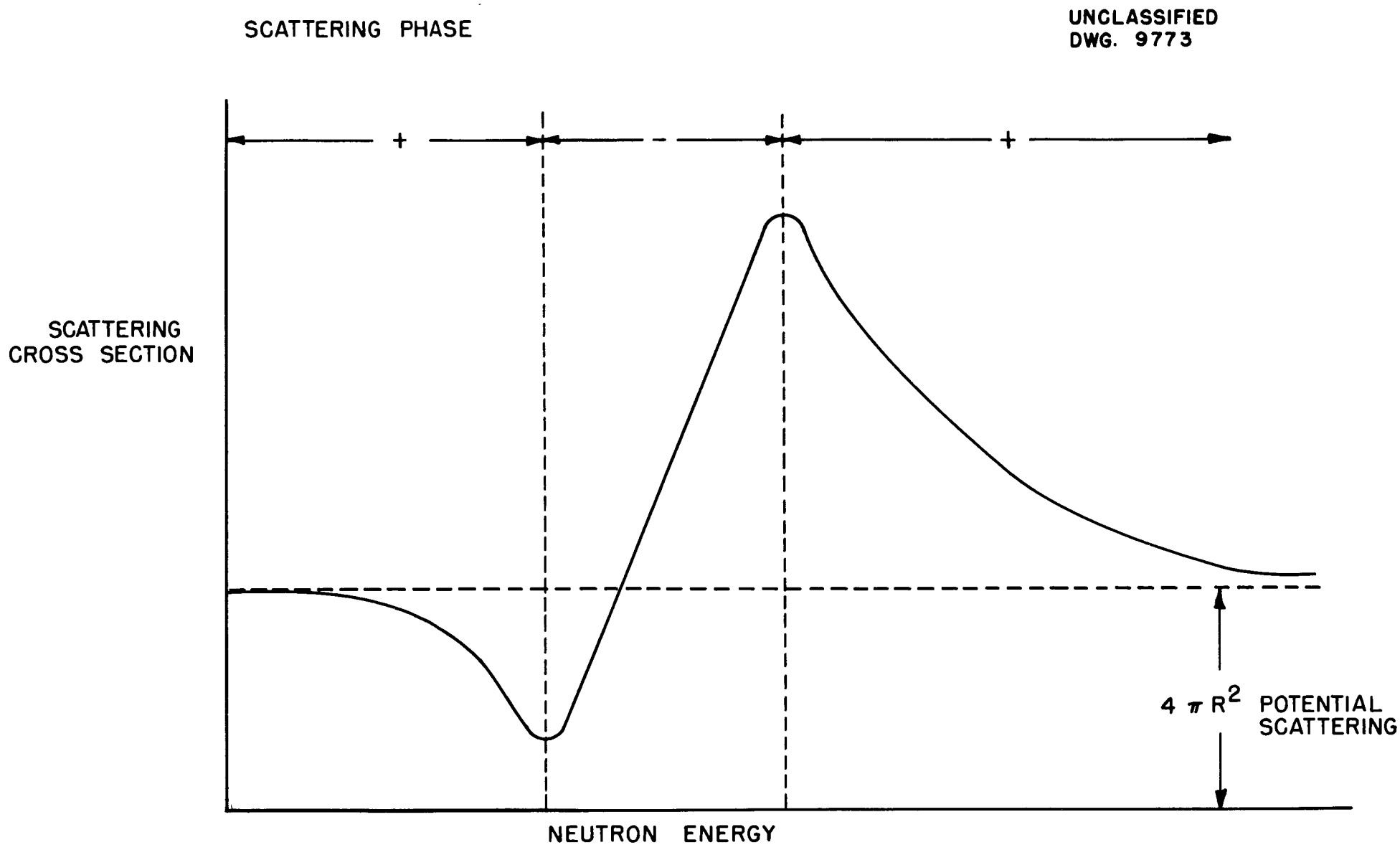

SCATTERING RESONANCE

FIG. 20

The fact that Ni^{58} scatters with positive phase plus the fact that its scattering cross section is considerably greater than the calculated potential scattering value suggests the existence of a scattering resonance peak in Ni^{58} at either positive neutron energies lower than any for which measurements were taken or at negative energies.

The diffraction peaks for $Ni^{60}O$ though present were much less pronounced than those for $Ni^{58}O$, corresponding to a much smaller scattering cross section. This agrees with the earlier statement that Ni^{58} was responsible for the high scattering cross section found in normal nickel. Due to the greater difficulty in plotting out these small discontinuities and since the correction for water content becomes comparable to the cross section left for $Ni^{60}O$, this curve was investigated less thoroughly. If Figure 19 is corrected for the oxygen cross section of roughly 4 barns one has no cross section left to attribute to the Ni^{60}. Obviously the correction made for water content was too large. The measurement of water content is quite difficult for such minute quantities of material and its large cross section demands great accuracy of measurement. However, it is quite certain from the data that the scattering cross section of Ni^{60} is less than the calculated potential scattering of 5.3 barns. The data are insufficient to determine the scattering phase but reference to Figure 20 suggests the possibility of a nearby resonance at a higher energy.

BIBLIOGRAPHY

BIBLIOGRAPHY

Amaldi, E. and Cacciapuoti, B. N. "On the Dependence of Nuclear Radius on the Mass Number," *The Physical Review,* 71:739, 1947.

Borst, L. B., Ulrich, A. J., Osborne, C. L. and Hasbrouck, B. "Diffraction of Neutrons and Neutron Absorption Spectra," *The Physical Review,* 70:108, 1946.

Buerger, Martin. *X-Ray Crystallography.* New York: John Wiley and Sons, 1942.

Compton, A. H. and Allison, S. K. *X-Rays in Theory and Experiment.* New York: D. Van Nostrand Company, Inc., 1935.

Du Mond, J. W. M. and Kirkpatrick, H. A. "The Multiple Crystal X-Ray Spectrograph," *Review of Scientific Instruments,* 1:88, 1930.

Fermi, E. and Marshall, L. "Interference Phenomena of Slow Neutrons," *The Physical Review,* 71:666, 1947.

Feshbach H., Peaslie, D. C. and Weisskopf, V. F. "On the Scattering and Absorption of Particles by Atomic Nuclei," *The Physical Review,* 71:145, 1947.

Goldsmith, H. H., "Neutron Cross Sections of the Elements," *Reviews of Modern Physics,* 19:268-82, 1947.

Halpern, O., Hamermesh, M. and Johnson, M. H., "The Passage of Neutrons Through Crystals and Polycrystals," *The Physical Review,* 59:981, 1941.

Handbook of Chemistry and Physics. Cleveland, Ohio: Chemical Rubber Publishing Company, 1949, 31st Ed.

Johann, H. H. "Die Erzeugung lichtstarker Rontgenspektren eit Hilfe von Konkavkristallen," *Zeitschrift Fur Physick,* 69:185, 1931.

Koehler, W. C., Wollan, E. O. and Shull, C. G. "The Coherent Scattering Cross Section of Nickel and Its Isotopes," *The Physical Review,* In Press.

Melkonian, E. "Slow Neutron Velocity Spectrometer Studies of O_2, N_2, A, H_2, H_2O and Seven Hydrocarbons," *The Physical Review,* 76:1750, 1949.

Meyer, C. F. *The Diffraction of Light, X-rays and Material Particles.* Chicago, Illinois: The University of Chicago Press, 1934.

Pomerance, H. and Hoover, J. I. MDDC-1626, p. 8., 1947.

Rainwater, L. J., Havens, W. J., Wu, C. S. and Meaker, C. L. *Reviews of Modern Physics,* 19:276, 1947.

Rose, M. E. and Shapiro, M. M. "Statistical Error in Absorption Experiments," ORNL-52, p. 6.